

**DEVELOPMENT OF A VORTEX GENERATING FLUME FOR THE REMOVAL OF
PHOSPHORUS FROM WASTE STREAMS**

by

RUSS R. McDONALD
B.S., University of California - Davis, 2001

A REPORT

submitted in partial fulfillment of the requirements for the degree

MASTER OF SCIENCE

Department of Chemical Engineering
College of Engineering

KANSAS STATE UNIVERSITY
Manhattan, Kansas

2007

Approved by:

Major Professor
Dr. Larry A. Glasgow

ABSTRACT

Feedlots, animal production facilities, and agricultural lands are point and non-point sources for nutrient enrichment of surrounding waterways and result in human enhanced eutrophication. Artificial elevation and increased enrichment from animal wastes, fertilizer, and runoff greatly increase the speed of this natural process and leads to degraded water quality, algae blooms, and fish kills. Phosphorous is typically the limiting nutrient for plant growth, and thus is the main focus of this paper. Phosphates enable excessive and choking plant growth that lead to depleted dissolved oxygen and excessive decaying plant matter, subsequently damaging the aquatic ecosystem.

In order to provide an inexpensive and feasible solution to minimize phosphate eutrophication, a passive, vortex generating flume has been proposed to provide the necessary mixing for the removal of phosphorus from waste waters. Preliminary tests with dye tracers and electrolyte pulse injections have been conducted to model the flow characteristics and determine the residence time under a variety of flow conditions, angle of inclination and flow rate.

The flume was modeled by two methods: four continuously stirred tank reactors (CSTRs) in series and as four CSTRs in series operating in parallel with a plug flow reactor (PFR). The hydraulic model fit a total of five parameters to the experimental data: Residence time, the inlet concentrations of the electrolyte pulse tracer, and the injection times of the tracer to both types of reactors.

The kinetic model was built based on data collected from a different study of swine lagoons using magnesium chloride to precipitate phosphorus as the mineral struvite. The precipitation kinetics were modeled using first order and irreversible reaction and incorporated into the hydraulic model. The vortex generating flume provided an operating space that sufficiently removed phosphorus from the waste stream. Future work will include pilot scale testing of the model using waste streams and the investigation of a scour to minimize solid formation in the flume.

TABLE OF CONTENTS

<u>Table of Contents</u>	<u>iii</u>
<u>List of Figures</u>	<u>iv</u>
<u>List of Tables</u>	<u>v</u>
<u>Acknowledgements</u>	<u>vi</u>
Chapters	
<u>1. Introduction</u>	<u>1</u>
<u>2. Hydraulic Model</u>	<u>5</u>
2.1 Introduction	5
2.2 Methodology	6
2.3 Hydraulic Model	8
2.4 Results	12
2.5 Discussion and Conclusions	26
<u>3. Kinetic Model</u>	<u>29</u>
3.1 Introduction	29
3.2 Methodology	31
3.3 Kinetic Model	32
3.4 Results	33
3.5 Discussion and Conclusions	39
<u>4. Discussion and Conclusions</u>	<u>41</u>
<u>References</u>	<u>44</u>
<u>Appendix</u>	<u>46</u>

LIST OF FIGURES

Figure 1.1	Water based phosphorus cycle	2
Figure 2.1	Diagram of vortex generating flume with dye tracer	5
Figure 2.2	Schematic of four tanks in series model	6
Figure 2.3	Schematic of four serial tanks in parallel with a PFR model	8
Figure 2.4	Characteristic plot of outlet conductivity of the flume	9
Figure 2.5	Bypass flow of dye tracer in the vortex generating flume	10
Figure 2.6	Velocity profile in single segment of the flume	11
Figure 2.7	Plot of tanks in series to model PFR portion of the flume	12
Figure 2.8	Characteristic plot of outlet conductivity and predicted vs. actual	14
Figure 2.9	Comparison of 4 CSTRs versus 4 CSTRs and 1 PFR models	16
Figure 2.10	Outlet conductivity and predicted vs. actual for 5.52 degrees and 1.1 lpm	18
Figure 2.11	Outlet conductivity and predicted vs. actual for 10.7 degrees and 1.1 lpm	19
Figure 2.12	Outlet conductivity and predicted vs. actual for 10.7 degrees and 1.1 lpm	21
Figure 2.13	Fitted values for residence time for CSTRs and PFR	23
Figure 2.14	Contour plots for CSTR and PFR residence times versus flow and angle	24
Figure 2.15	Ratio of inlet concentrations of PFR:CSTR versus flow rate and angle	25
Figure 2.16	Outlet conductivity and predicted vs. actual for 4.36 degrees and 2.24 lpm	26
Figure 3.1	Solubility of metal phosphates	29
Figure 3.2	Dissolved phosphate concentrations in anaerobic swine lagoons	30
Figure 3.3	Affects of pH and Mg:P ratio on phosphate removal	31
Figure 3.4	Contour plots of outlet phosphate concentration for $C_{in}=63.8\text{mg/L}$	35
Figure 3.5	Contour plots of outlet phosphate concentration for $C_{in}=540\text{mg/L}$	36
Figure 3.6	Contour plots of outlet phosphate concentration for $C_{in}=540\text{mg/L}$	38

LIST OF TABLES

Table 1.1	Probable sources contributing to water quality impairment in Kansas	4
Table 1.2	Causes of water quality impairment in Kansas	4
Table 2.1	Operating conditions of vortex generating flume	6
Table 2.2	r^2 values for four tanks in series model correlation to the data	13
Table 2.3	Values for five parameter model and r^2 -adjusted	15
Table 2.4	Volumetric capacity for phosphate precipitating flume	28
Table 3.1	Conversion of soluble to precipitated phosphates	34

ACKNOWLEDGEMENTS

With the completion of this report, I am one step closer to completing the requirements for a Masters Degree. Amidst a balancing act of family, work, and the pursuit of an advanced degree it has been an exciting, rewarding, and satisfying journey.

I wish to begin by thanking all of the individuals responsible at Kansas State University for the development and implementation of a graduate engineering distance education program. A special thanks to Dr. James Edgar, Dr. Larry Glasgow, Dr. Keith Hohn, and Dr. Jennifer Anthony who have provided guidance along the way and helped shape my program of study. I would also like to thank all the undergraduate students working for Dr. Glasgow on this project. In addition, without the dedication of the staff in the Division of Continuing Education and my many exam proctors at Newberg Public Library, none of this would have been possible.

I am grateful for the continued support that friends and family have provided along the way. A special thanks to my wife and daughter for their support throughout my studies and to my grandfather who inspired me to pursue a course of study in engineering.

CHAPTER 1 - INTRODUCTION

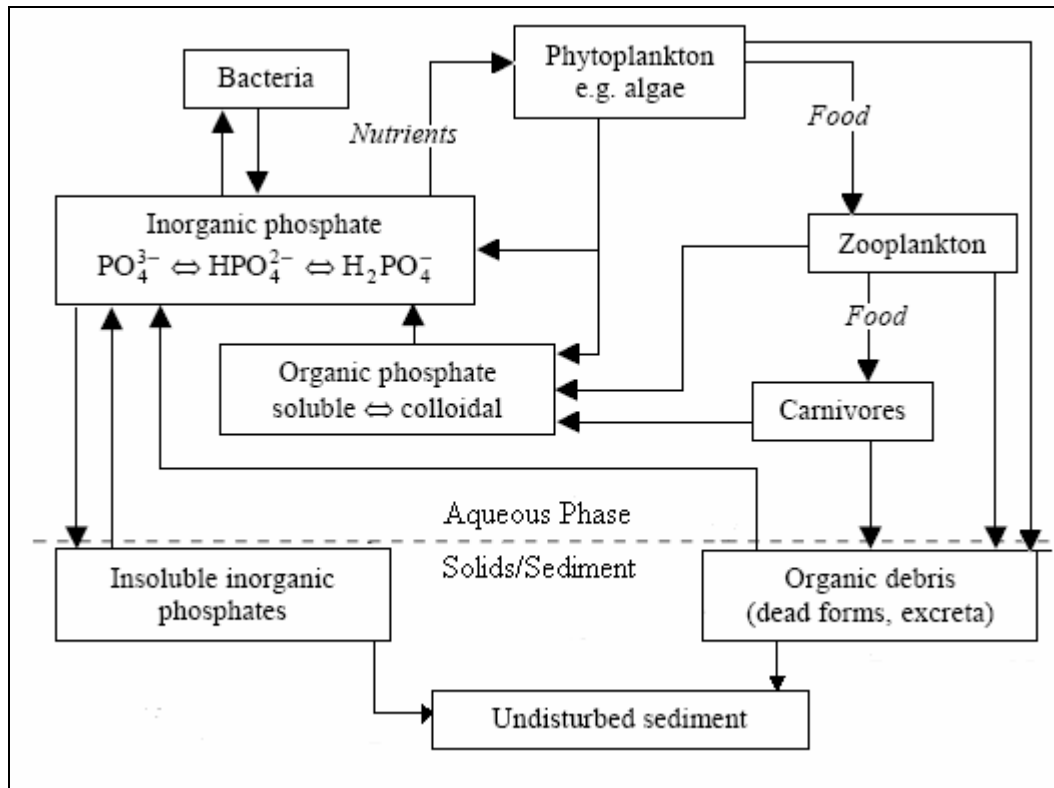
Eutrophication is the natural aging process of lakes and streams, which normally occurs over many centuries. It can, however, be rapidly accelerated by human activities. It is predominantly driven by pollution from an overabundance of nitrogen and phosphorus, leading to rapid and excessive plant growth and decay.

Eutrophication can lead to severe reductions in water quality and usability that are characterized by aggressive growth of waterway-choking plant life, toxic algal blooms, dissolved oxygen depletion, and consequent harm to native species of plants and animals. Additional impacts of cultural eutrophication range from reduced availability of untreated drinking water to a decline in the aesthetic and recreational value of water bodies world wide. It can lead to disruption and even destruction of ecosystems. A survey by the International Lake Environment Committee (1993) found that 54% of lakes in Asia are eutrophic, 53% in Europe, 48% in North America, 41% in South America, and 28% in Africa. Although eutrophication has been identified as a problem in North American and European lakes since the mid 20th century (Rodhe, 1969), developing countries are now beginning to address similar problems.

Phosphorus is typically the limiting nutrient in plant growth and is commonly considered to be the primary pollutant leading to eutrophication. Approximately eight times more nitrogen is required for plant growth than phosphorus (UNEP, 2002). Typical phosphorus sources include fertilizers, manures, sewage, detergents, and wastewater that is incorporated into runoff and finally deposited into bodies of water. From 1950 to 1995, 600 million metric tons of phosphorus were consumed globally, the bulk of which was applied to croplands (Carpenter et al, 1998). Human activities on this scale are the main driving force behind the increase in eutrophic bodies of water around the world. An example is Lake Süsser See in the Mansfeld Lake Basin in northeastern Germany. Since the 1950's the lake has experienced reduced water quality and an overall reduction in aquatic life. Alum treatments have been employed to reverse the damage from eutrophication by precipitating the phosphorus. A total of 7000 tons of alum was applied between 1977 to 1992 (Lewandowski et al, 2003) to the lake to reduce phosphorus concentrations with limited success. Figure 1.1 adapted from Reddy, (1998) shows the

water based phosphorus cycle. As noted in the cycle shown below, the two exit points for phosphorus from the cycle are the insoluble inorganic phosphates and undisturbed sediment. The focus of this paper will be on the removal of phosphorus from liquid waste streams from intensive livestock operations (e.g. feedlots) as precipitated inorganic phosphates.

Figure 1.1: Water based phosphorus cycle (Reddy et al, 1998).



In the United States, as it is world wide, agricultural production is a main contributor to phosphorus migration and cultural eutrophication. Phosphorus sources range from fertilized farmlands, erosion, concentrated animal production operations, and runoff. The US Department of Agriculture originally recommended controls and safeguards on the effects of nitrogen runoff and enrichment when eutrophication was first being addressed. In subsequent years, the efforts have shifted to an overall nutrient management plan instead of focusing public efforts on nitrogen as a single source (Sharpley et al, 1999). Current remediation efforts range from buffer zones between croplands (and other point sources) and bodies of water to advanced biological/chemical reactors to bind the soluble phosphorus and use the output as a time-release fertilizer.

Regardless of the methodology, two factors are paramount in the successful adoption of nutrient enrichment mitigation: economic impact and effectiveness. Currently, a common and cost-effective technique is to precipitate the phosphorus using readily available chemicals containing calcium, aluminum, or iron. The resulting precipitates all have relatively low solubility when bound with phosphate and are relatively inexpensive. However, solubility can greatly vary as a function of pH. An alternative method is to precipitate phosphate and ammonia simultaneously as struvite, $\text{MgNH}_4\text{PO}_4 \cdot 6\text{H}_2\text{O}$, by using magnesium chloride. This technique is also relatively inexpensive, however it is sensitive to the pH of the solution. Yang et al (2006) found that a range in pH of 7.5 to 11.8 for an equi-molar solution of Mg:P changed the removal of total phosphorus from approximately 65% to 95% removed. Similarly, Celen and Buchanan et al (2007) found that the phosphate concentration of Mg treated waste water at a pH of 6.84 dropped from 234 (+/-6) mg/L to 8 (+/-4) mg/L when the pH was increased to 8.5.

Current processes for reversing eutrophication are chemical treatment and precipitation, activated sludge removal, dredging of nutrient rich sediment, bio-manipulation, and possibly coupling these processes with biological reduction measures. In addition to remediation efforts, preventative measures are key to reducing eutrophication. In Kansas alone, greater than 50% of impaired waters have been affected by agricultural type sources. Nutrient enrichment alone from these sources predominantly affects stagnant bodies of water such as lakes, ponds, and wetlands. Table 1.1 and 1.2 below provide the estimated breakdown.

Table 1.1: Probable sources contributing to water quality impairment in Kansas. Report 305(b)US EPA, 2004.

Source Name	Rivers, Streams, Creeks (Miles)	Lakes, Ponds, Reservoir (Acres)	Wetlands (Acres)	% Rivers, Streams, Creeks (Miles)	% Lakes, Ponds, Reservoir (Acres)	% Wetlands (Acres)
AGRICULTURE	9743	156847	25435	15.3%	81.9%	51.0%
CROP PRODUCTION (CROP LAND OR DRY LAND)	5199	0	0	8.2%	0.0%	0.0%
INTENSIVE ANIMAL FEEDING OPERATIONS	6641	0	0	10.4%	0.0%	0.0%
IRRIGATED CROP PRODUCTION	4003	0	0	6.3%	0.0%	0.0%
LIVESTOCK (GRAZING OR FEEDING OPERATIONS)	7790	0	0	12.3%	0.0%	0.0%
NON-IRRIGATED CROP PRODUCTION	4159	0	0	6.5%	0.0%	0.0%
ALL OTHER SOURCES	26056	34762	24421	41.0%	18.1%	49.0%
TOTAL	63591	191609	49856	100%	100%	100%
% from Agriculture/Farming & Animal Production	59.0%	81.9%	51.0%			

Table 1.2: Causes of water quality impairment in Kansas. Report 305(b)US EPA, 2004.

Water Body	Impairment Description	Total Miles or Acres affected	Impaired Waters, State Total	%
Lakes, Ponds, & Reservoirs	EUTROPHICATION (NUTRIENTS/CHLOROPHYLL-A/TROPIC STATE)	146,209	304547	48.0%
Rivers & Streams	NUTRIENTS	346	15560	2.2%
Wetlands	EUTROPHICATION (NUTRIENTS/CHLOROPHYLL-A/TROPIC STATE)	26,484	102565	25.8%

The main focus of this report will be the investigation of a vortex generating flume used for cost-effective treatment of P-bearing wastewaters; the system is intended specifically for agricultural and animal production run-off.

CHAPTER 2 - HYDRAULIC MODEL

Introduction

Phosphorus precipitation efforts rely on adequate mixing to insure the maximum removal of soluble phosphorus is achieved in order to limit the negative effects of eutrophication. In an effort to keep treatment costs to a minimum, a vortex generating flume has been proposed as a passive mixing device. See Figure 2.1 below for a pilot scale model of the flume.

Figure 2.1: Vortex generating flume with four identical sections. Inlet is shown on the left, direction of flow is to the right. A total of four vortex generating regions are in the flume.



As can be seen from the purple dye pulse tracer, vortices are formed in each section of the flume. The strength of a vortex is proportional to the velocity of the fluid. The higher flow rates provide stronger vortices; however, the increase in flow rate also reduces the overall residence time of the system in which the reaction(s) occurs.

In this study, conductivity data have been collected in order to characterize the flow in this type of flume by determining the residence time distribution. Additionally, the volume of each vortex generating flume segment was determined as a function of the angle of inclination (data in Appendix). A concentrated pulse injection of sodium chloride (10mL of 10g NaCl in 200mL H₂O) has been applied to the inlet of the flume and the subsequent downstream conductivities measured. The experimental apparatus used a OAKTON conductivity meter and a calibrated rotameter. The conductivity data were then normalized to the baseline conductivity. For conditions where the baseline was noisy or appeared to be drifting, an average of the baseline was used to normalize the conductivity data. Flow calibration data are shown in the Appendix. A range of angles and inlet flow

rates was employed to model the effects of mean residence time and mixing. Table 2.1 provides the pilot settings of the flume.

Table 2.1: Operating conditions of vortex generating flume.

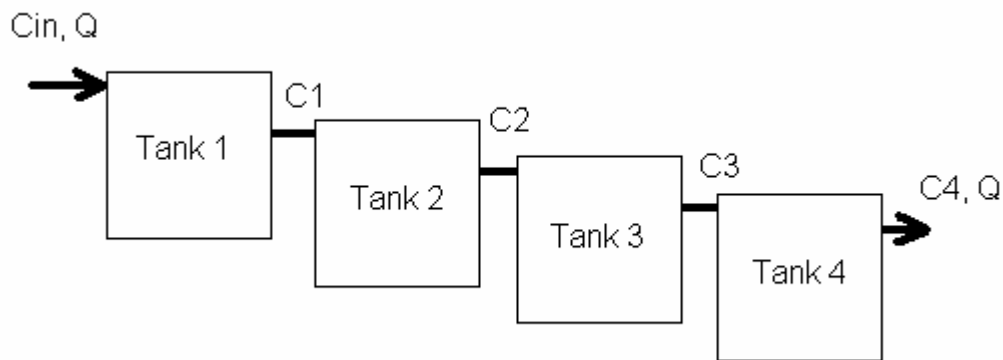
Angle (Deg.)	4.36	4.36	4.36	5.19	5.19	5.19	7.74	7.74	7.74
Flow (LPM)	1.1	2.24	3.45	1.1	2.24	3.45	1.1	2.24	3.45
V_i (L)	0.715	0.715	0.715	0.660	0.660	0.660	0.395	0.395	0.395
Angle (Deg.)	5.52	5.52	5.52	10.7	10.7	10.7			
Flow (LPM)	1.1	2.20	3.30	1.1	2.20	3.30			
V_i (L)	0.700	0.700	0.700	0.335	0.335	0.335			

Angles greater than 10.7 degrees were not considered in this study due to the probable topology of the sites in which flumes might be utilized. In fact, some sites may require even smaller angles of inclination, well below 4.36 degrees.

Methodology

The vortex generating flume was modeled using continuously stirred tank reactors (CSTRs) in series. A schematic of the reactors used to model the flume is shown below, in Figure 2.2.

Figure 2.2. Model schematic of reactors for vortex generating flume.



The mass balance on a CSTR is of the form:

$$Q * C_{i-1} - Q * C_i = V_i * \frac{dC_i}{dt} \quad (1)$$

where C_i is the concentration of in tank i , V_i is the volume of tank i , and Q is the steady state volumetric flow rate. The reaction will be discussed in the next section. Each segment is assumed to have the same volume and be well mixed, hence $V_i=V$. To incorporate the residence time into the mass balance, substitute

$$\tau = V/Q \quad (2)$$

into equation 1 to yield:

$$\frac{dC_i}{dt} = \frac{1}{\tau} * (C_{i-1} - C_i). \quad (3)$$

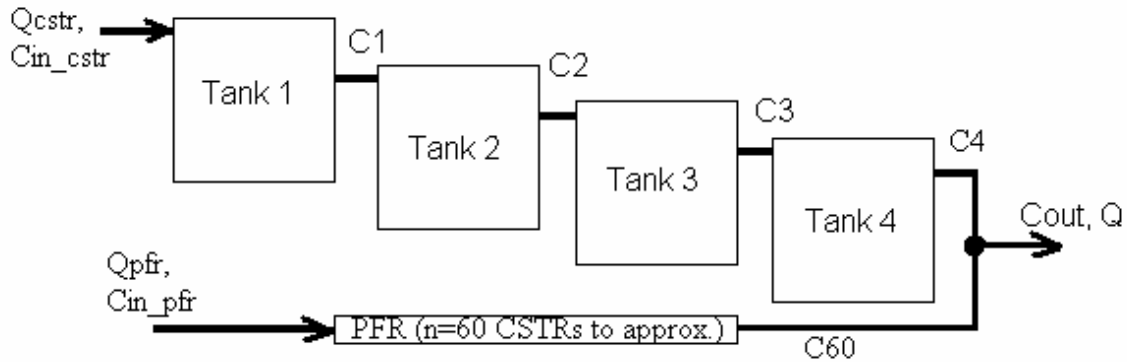
The model was discretized and a characteristic time step of 0.1 seconds was used to model the system in Excel. Using a first order forward difference to approximate the derivative, with a j index to represent the time step, leads to the discretized mass balance of the i^{th} tank for the $j+1$ time index shown in equation 4:

$$C_{i,j+1} \cong \frac{\Delta t}{\tau} * (C_{i-1,j} - C_{i,j}) + C_{i,j}. \quad (4)$$

Data were manually collected using a stopwatch and conductivity measurements in the first region of the flume (tank 1) and the fourth region of the flume (tank 4). Conductivity data were collected at 5 second intervals. The model was compared to laboratory data. The conductivity data were normalized to a baseline value.

An alternative model for the system was formulated for higher flow rates with the four CSTRs in series and an additional plug flow reactor (PFR) in parallel operation. The reasoning for this type of system will be discussed later. See the schematic below, in Figure 2.3, for the alternate reactor configuration. In Excel, the PFR was modeled by using 60 small tanks in series and the same general form of the mass balance was used as shown in equation 4.

Figure 2.3. Alternate reactor configuration for modeling vortex generating flume.



Excel data analysis and parameter estimation were performed using the Solver feature in order to minimize the sum of squares error between the predicted outlet concentration of the model and the collected data. Practical constraints were included; for example, both the residence time and injection concentration had to be greater than zero. Injection time (pulse duration) was estimated to be between 0.5 and 2 seconds and limited to this range of values. For the reactor scheme including the parallel operation of a PFR, the residence time of the PFR and injection concentration values were constrained to being less than the values for the four CSTRs in series. The predicted values of the outlet concentration were plotted against the collected data. The statistics r^2 and r^2 -adj were used to evaluate the overall agreement between the model and the data sets. SAS-JMP was also used to generate contour plots of the collected data.

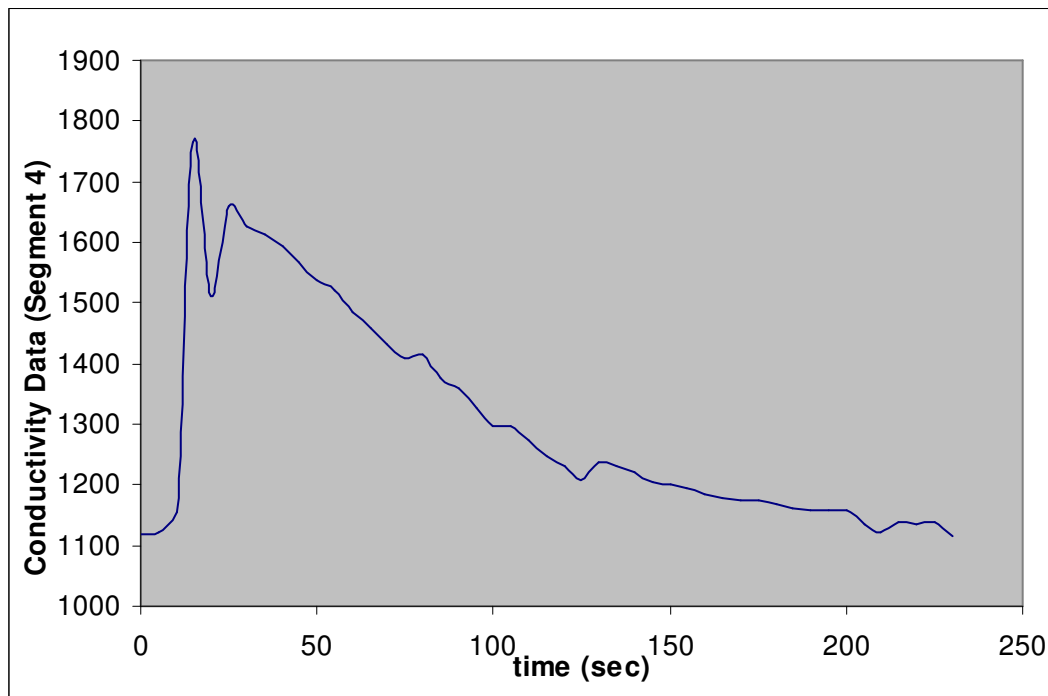
Hydraulic Model

The electrolyte data were fit to a model that was based on four continuously stirred tank reactors (CSTRs) in series. Conductivity data from the sodium chloride pulse tracer were measured in the uppermost and lowermost regions of the flume, segments 1 and 4, respectively. This study predominantly focuses on the output and analysis of the last tank in the flume, since this is the parameter of interest in predicting the effectiveness of the flume for precipitating phosphates from solution. The four CSTR model used the residence time, injection concentration, and injection time as adjustable parameters. The assumptions employed are CSTR behavior (the contents of the tank are well mixed and the outlet concentration is the same as the bulk concentration within the reactor). For angles of inclination of approximately 7 degrees or less and flow rates of 1.1 lpm or less, the four

CSTR model fit the data well with $r^2 > 0.90$ for predicted versus actual concentrations. However, for flow rates above 1.1 lpm and angles greater than approximately 7 degrees, the four CSTRs in series model ranged from fitting the pilot data semi-quantitatively ($r^2 \sim 0.75$) to poorly ($r^2 < 0.6$).

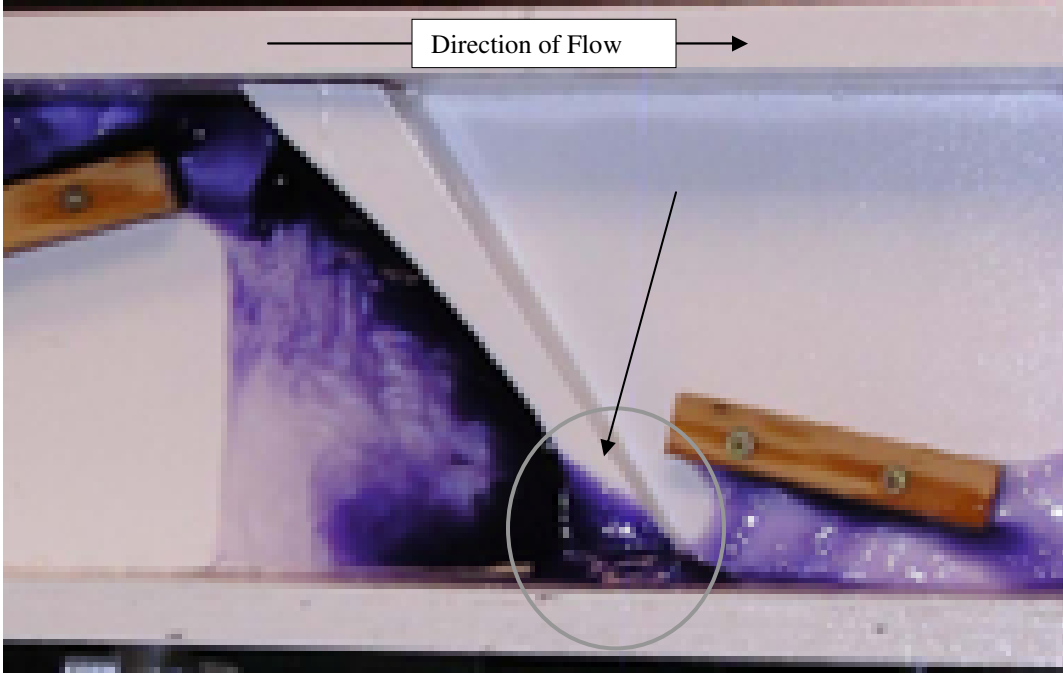
A characteristic of the data sets not well fit by the four CSTR model was a sharp spike or peak relatively early in the outlet concentration of the flume. This suggests that the four tanks in series model cannot adequately represent the data. The spike in conductivity is suggestive that a PFR added in series may better describe the flow characteristics of the flume and will be discussed later in this section. Figure 2.4 is representative of this type of behavior.

Figure 2.4. Representative trace of outlet conductivity. Note the characteristic peak in conductivity on the flume outlet (segment 4, 5.19 deg, 3.45 lpm).



In addition to this characteristic behavior in certain data sets, it was observed when using a dye pulse tracer in the flume that some portion of the flow appeared to move through the flume much faster than the well mixed bulk of the flow. Figure 2.5 shows a close-up of the second region of the flume, tank 2.

Figure 2.5: Close-up of second region of the flume, approximated by the second CSTR in series. Note the variation in the dye concentration of the outlet versus the bulk dye concentration in the vortex generating portion.



As can be seen in the photo of the flume above, some portion of concentrated purple dye is able to spill over the individual weir, escape, and adversely affect the mixing in each segment of the flume. Qualitatively, this is intuitive since the surface velocity is the highest velocity in the flume and will travel through the flume in the shortest period of time. This can be shown by developing a relatively simple two dimensional model for the velocity in an individual segment of the flume. The velocity for two dimensional flow is given by the equation

$$\frac{\partial^2 V_z}{\partial x^2} + \frac{\partial^2 V_z}{\partial y^2} = -\frac{\rho g \sin \theta}{\mu}, \quad (5)$$

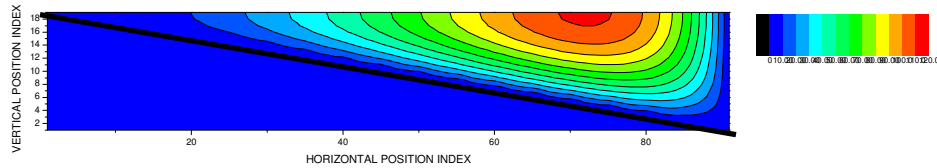
which can be discretized and solved for the velocity, $V_{i,j}$, leading to:

$$V_{i,j} = \frac{1}{4} * \left(V_{i+1,j} + V_{i-1,j} + V_{i,j+1} + V_{i,j-1} + \frac{\Delta x^2 * \rho * g_z * \sin \theta}{\mu} \right). \quad (6)$$

The horizontal (x) index is i, the vertical (y) index is j, and $V_{i,j}$ is the fluid velocity for the point (i,j). Figure 2.6 below shows the velocity contour plot and indicates that the

maximum velocity is approximately 120 cm/s and occurs at the free surface, approximately 3 cm upstream of the weir.

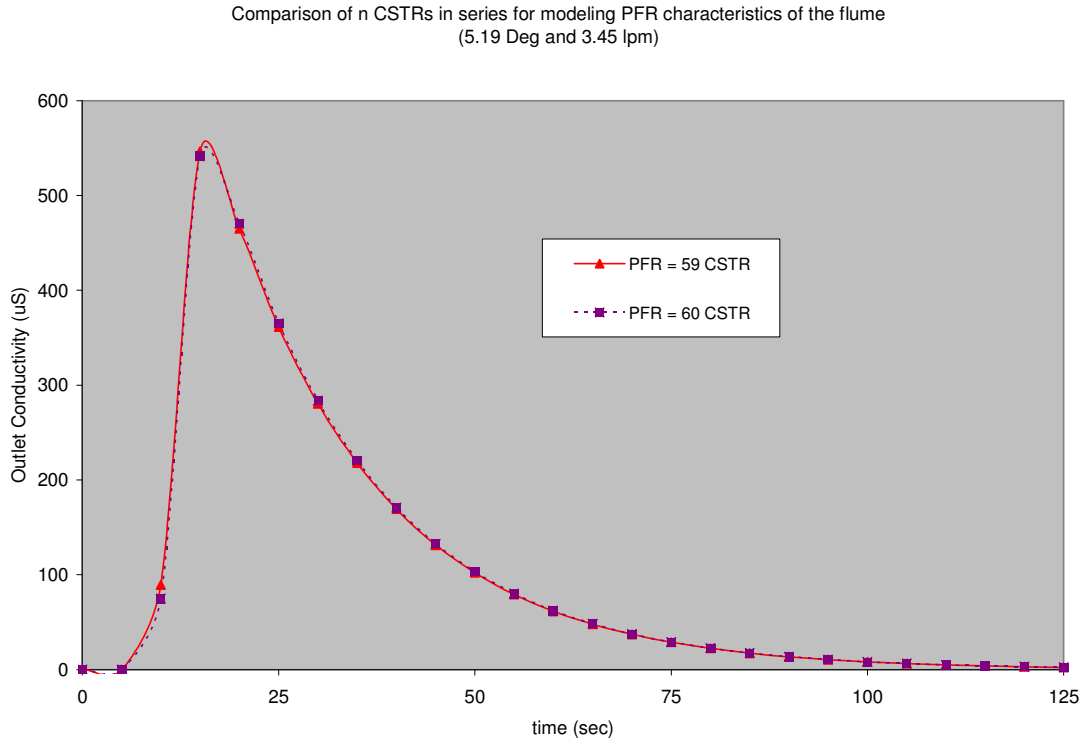
Figure 2.6: Velocity (cm/s) contour for single flume segment where the channel width is 15.24 cm, the maximum depth is 3.05 cm, and $(\rho^*g^*\sin\theta)/\mu = 49$.



Based on the observations and consistent data sets that demonstrate this behavior, it was considered that there may be some form of short-circuiting or bypass behavior that was not accounted for by using a four CSTRs in series model.

From a modeling perspective, it was considered that the bulk of the flow could still be adequately modeled by four CSTRs. As seen in the dye tracer pictures of the flume, the bulk of the flow appears well mixed. However, some bypass clearly occurs in which the solution quickly moves through the four segments of the flume, is not well mixed, and emerges relatively early at the outlet of the flume. Accordingly, the model was modified to incorporate a smaller PFR reactor in series with the four CSTRs reactors in series. The PFR was modeled as a series of sixty small CSTRs in series; this technique was used based on the relative simplicity and setup in Excel. Figure 2.7 below shows the delta between the values for fifty-nine CSTRs in series versus sixty CSTRs in series. As shown, the difference in the output of the PFR modeled by 59 versus 60 CSTRs in series is negligible (averages ~1% difference).

Figure 2.7: Comparison of n=59 and n=60 CSTRs in series to approximate the PFR portion of fluid flow.



The adjusted model used a total of five parameters to fit the data: mean residence times for both the PFR and four CSTRs in series, the pulse inlet concentrations, and the pulse injection time. The sum of squares error between the predicted values for the outlet conductivity versus the data values for outlet conductivity was minimized by determining the optimum values for the five parameter model. For most of the flume operating conditions, this enhancement to the model significantly increased the r^2 value between the model versus experimental values for the outlet concentration and will be discussed in the next section.

Results

In the initial analysis of the data the system was represented with four CSTRs in series. While this model was adequate for fitting the output of the flume at 1.1 lpm ($r^2 > 0.9$), it failed to adequately fit at higher values of flow, especially at the higher angles of inclination. Also of note, the model does not adequately describe the behavior for the entrance portion of the flume ($0.003 < r^2 < 0.875$). This study focused on the output of the

system versus the output of individual segments of the system. Table 2.2 below, shows agreement between the model and the data.

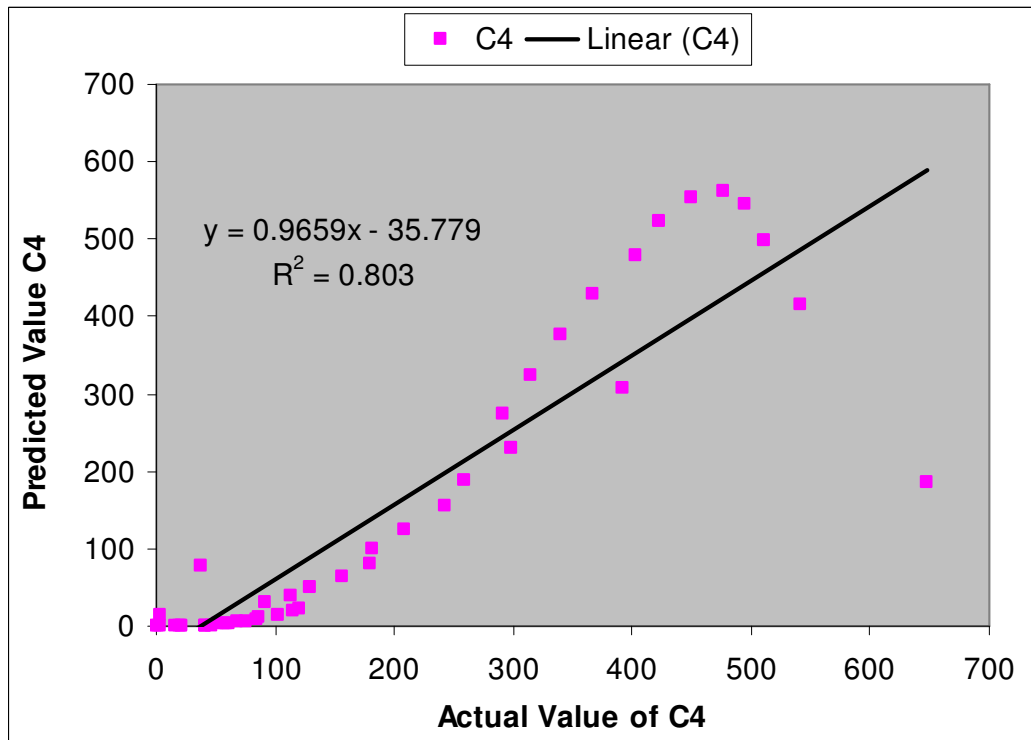
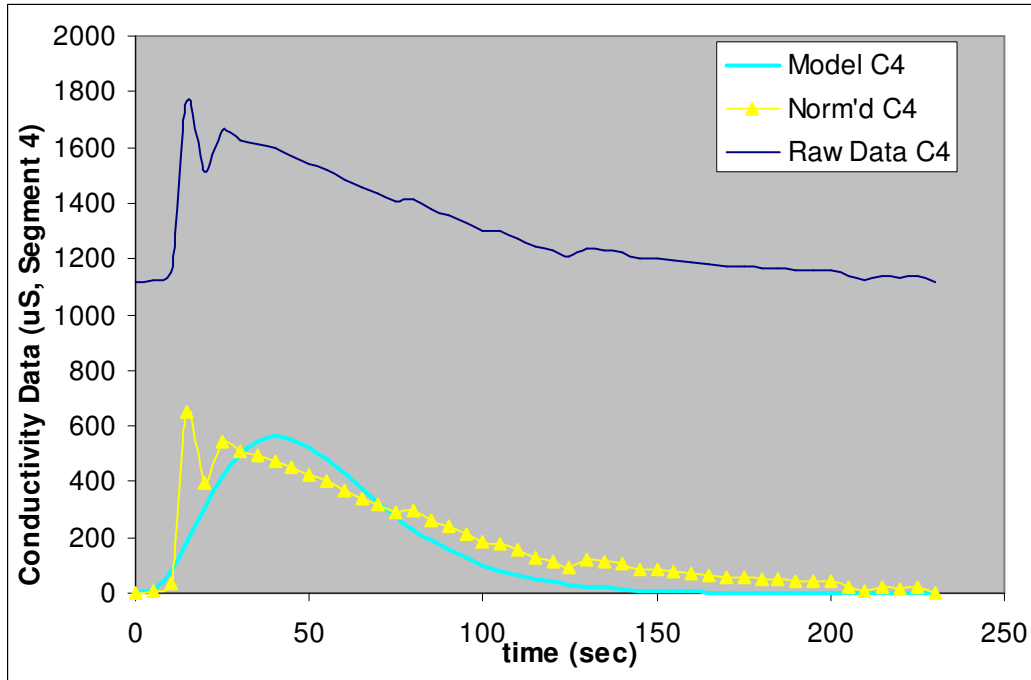
Table 2.2: r^2 for various flow conditions for predicted vs. actual outlet conductivity for the four CSTRs in series model.

Angle (Deg.)	Flow (LPM)	Vn (L)	Calculated Tau (s)	Fitted Tau (s)	Fitted Inj Time (s)	Fitted Cin (μ S)	r^2 for C1	r^2 for C4
4.36	1.1	0.715	39.0	32.0	1.0	69.5	0.279	0.942
4.36	2.24	0.715	19.2	14.6	1.0	38.9	0.799	0.778
4.36	3.45	0.715	12.4	15.3	1.0	33980.2	0.875	0.703
5.19	1.1	0.660	36.0	46.4	1.0	107056.6	0.003	0.914
5.19	2.24	0.660	17.7	17.2	1.0	51030.1	0.492	0.865
5.19	3.45	0.660	11.5	13.4	1.0	33514.7	0.461	0.804
7.74	1.1	0.395	21.5	46.6	1.0	210.9	0.110	0.971
7.74	2.24	0.395	10.6	13.1	1.0	54.8	0.017	0.891
7.74	3.45	0.395	6.9	9.8	1.0	33291.8	0.568	0.585

As shown, the four CSTR in series model can adequately represent the data for the lowest flow rate at all angles ($r^2 > 0.91$). However, as the flow rate increased beyond 1.1 lpm, the fit became qualitative at best. Most notably, the r^2 for an angle of 7.74 degrees and flow rate of 3.45 lpm only yielded a value of 0.585.

Figure 2.8 below illustrates the main discrepancy between the four CSTR model and the four CSTRs in series in parallel with a PFR. It is predominantly seen in the early portion of the outlet conductivity at the bottom of the flume and is characterized by a sharp peak and an inflection point in the concentration. In addition, the model systematically under-predicts the outlet concentration in the tail portion of the distribution. Based on the r^2 values, the overall fit of the model only accounts for 80% of the variation seen in the data.

Figure 2.8: Representative trace of outlet conductivity. (segment 4, 5.19 deg, 3.45 lpm).



When the data sets were fit to a four CSTR with parallel PFR, there was a notable increase in the model fit. Table 2.3 below provides r^2 values along with the estimated values of the five parameters used in the model.

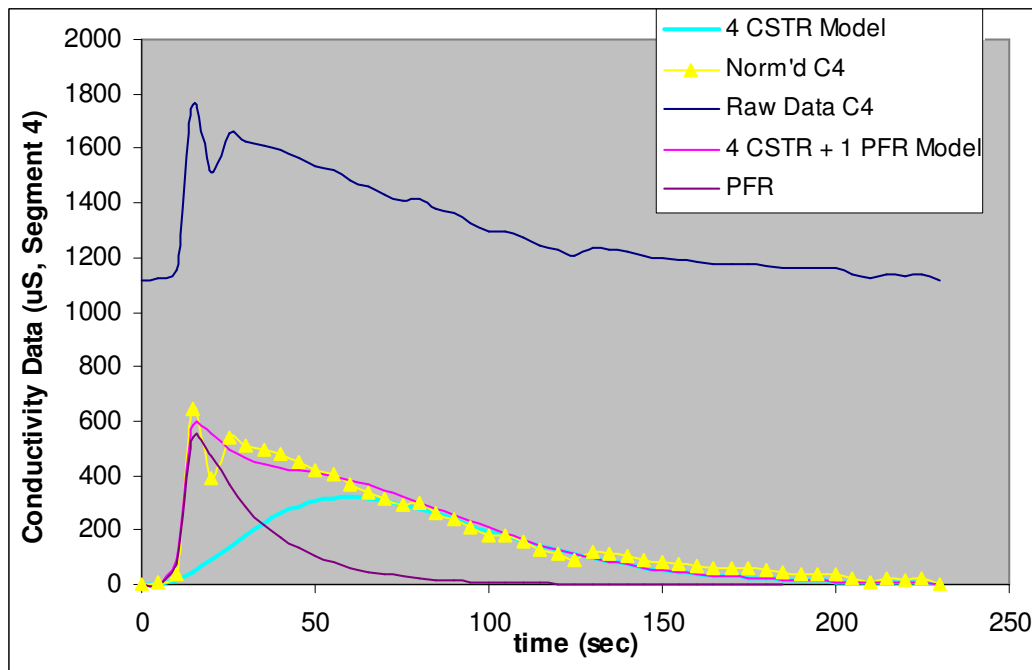
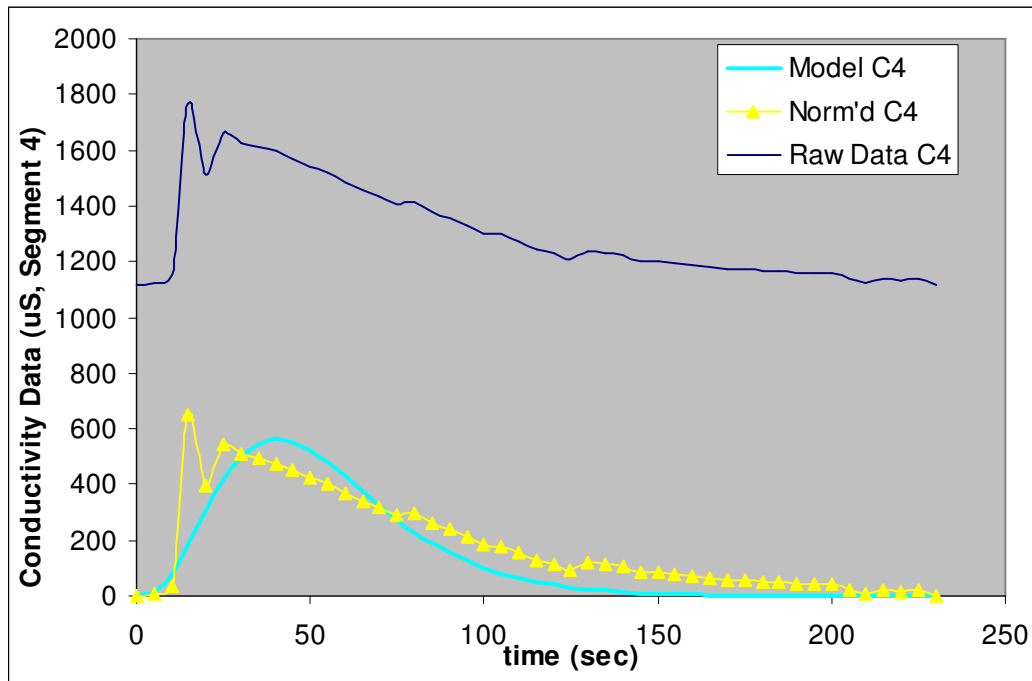
Table 2.3: Five parameter model results for four CSTR in series + 1PFR in parallel.

Angle (Deg.)	Flow (LPM)	Vn (L)	Fitted Inj Time (s)	Single CSTR Fitted Tau (s)	Tau of 4 CSTRs in Series (s)	CSTR Fitted Cin (μ S)	PFR Fitted Tau (s)	PFR Fitted Cin (μ S)	r ² for 5 param CSTR & PFR Model	r ² -Adj for 5 param CSTR & PFR Model
4.36	1.1	0.715	1.0	36	142	67	38	1	0.979	0.977
4.36	2.24	0.715	1.0	20	80	28	22	2	0.967	0.961
4.36	3.45	0.715	1.0	24	96	29477	18	1736	0.947	0.939
5.19	1.1	0.660	1.0	55	219	95869	56	3136	0.974	0.972
5.19	2.24	0.660	1.0	23	90	46141	19	1885	0.963	0.960
5.19	3.45	0.660	1.0	20	79	28318	19	1854	0.960	0.955
7.74	1.1	0.395	1.0	51	203	197	64	4	0.988	0.988
7.74	2.24	0.395	1.0	16	62	49	19	2	0.975	0.971
7.74	3.45	0.395	1.0	12	49	28849	14	1629	0.970	0.964*
5.52	1.1	0.700	1.0	68	272	130835	51	3410	0.888	0.881
5.52	2.2	0.700	1.0	23	92	35214	22	1597	0.976	0.972
5.52	3.3	0.700	1.0	17	67	27498	19	1443	0.960	0.954
10.7	1.1	0.335	1.0	42	168	97167	30	3429	0.854	0.843
10.7	2.2	0.335	1.0	12	47	43783	15	1662	0.992	0.990
10.7	3.3	0.335	1.0	8	33	35	5	2	0.967*	0.956**

*Note: 2 outliers omitted. **Note: 3 outliers omitted.

As shown, r² values are quite high, with most values greater than 0.95. A property of r²-adjusted is that it compensates for the number of parameters used to fit the model and can be used to directly compare models with different numbers of adjustable parameters. r²-adjusted was also found to be quite high, again with most greater than 0.95, suggesting that using a five parameter model was not inflating the model's goodness of fit to the data set. Figure 2.9 below, shows a representative data set in which the four CSTR model is compared to the four CSTR and one PFR in parallel model. Data sets for all additional conditions can be found in the Appendix.

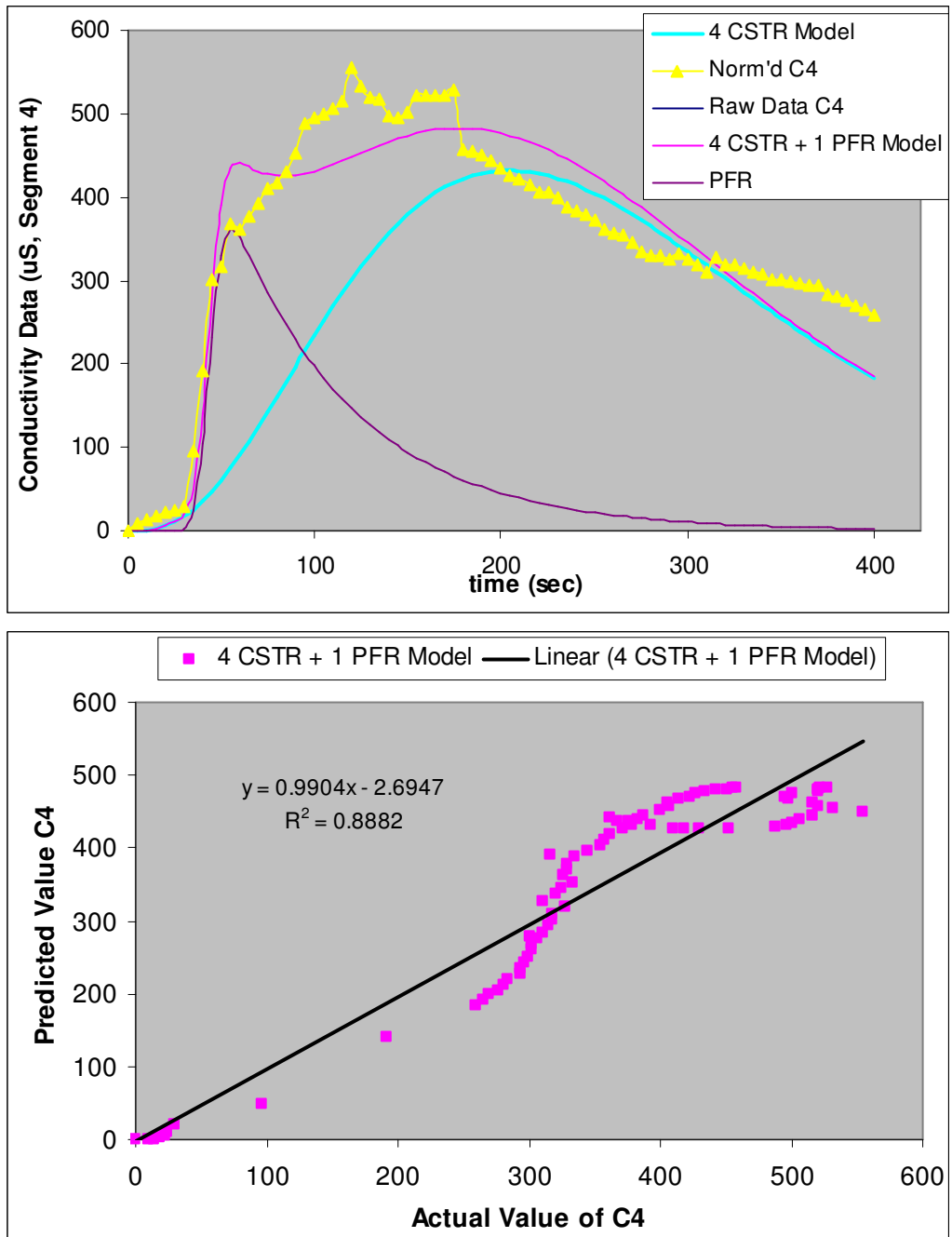
Figure 2.9: Comparison of fit for four CSTR model vs. four CSTR and 1 parallel PFR. r^2 values of 0.803 and 0.960, respectively. (segment 4, 5.19 deg, 3.45 lpm).



A total of three conditions did not yield r^2 or r^2 -adj values above 0.9. The 5.52 degree and 1.1 lpm flow is one such case. A shift in the data was observed and was only seen in this one trial suggesting a possible error in experiment execution; additional runs would need to be made at this condition to validate. Figure 2.10 shows the data details for

this trial. In order to better understand this condition and obtain a better fit, data should be collected over a longer period. In addition, some interesting behavior is observed in the predicted versus actual values obtained for conductivity in segment 4. The model initially under-predicts the conductivity (45 to 85 sec), then over-predicts (85 to 175 sec), under-predicts once again (175 to 310 sec), and finally over-predicts (310 to 400 sec). The oscillation in the model over or under-predicting the observed conductivity values is reflected in the unusual plot observed in figure 2.10.

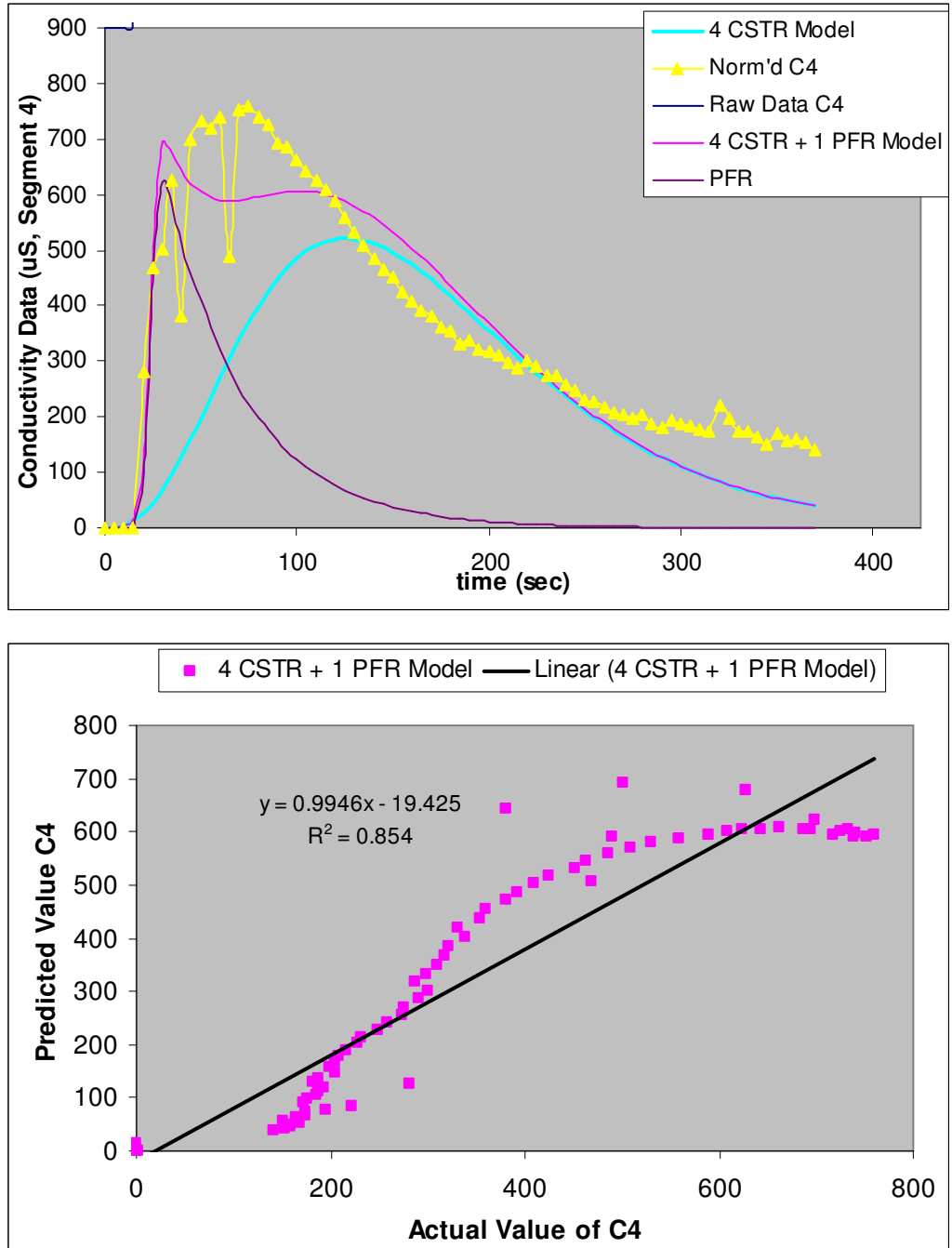
Figure 2.10: Observed outlet conductivity (segment 4, 5.52 deg, 1.1 lpm).



The 10.7 degree and 1.1 lpm flow: two outliers were observed in the data sets (sharp drops in conductivity). It is possible that there was an experimental error, or possibly some additional bypassing in which low conductivity flow preferentially made its way through the flume and caused a low spike in the conductivity readings. These points are also observed on the plot of predicted versus actual values of conductivity. Again,

further investigation with respect to these conditions would be required. Figure 2.11 shows the detailed data for this trial.

Figure 2.11: Observed outlet conductivity. (segment 4, 10.7 deg, 1.1 lpm).

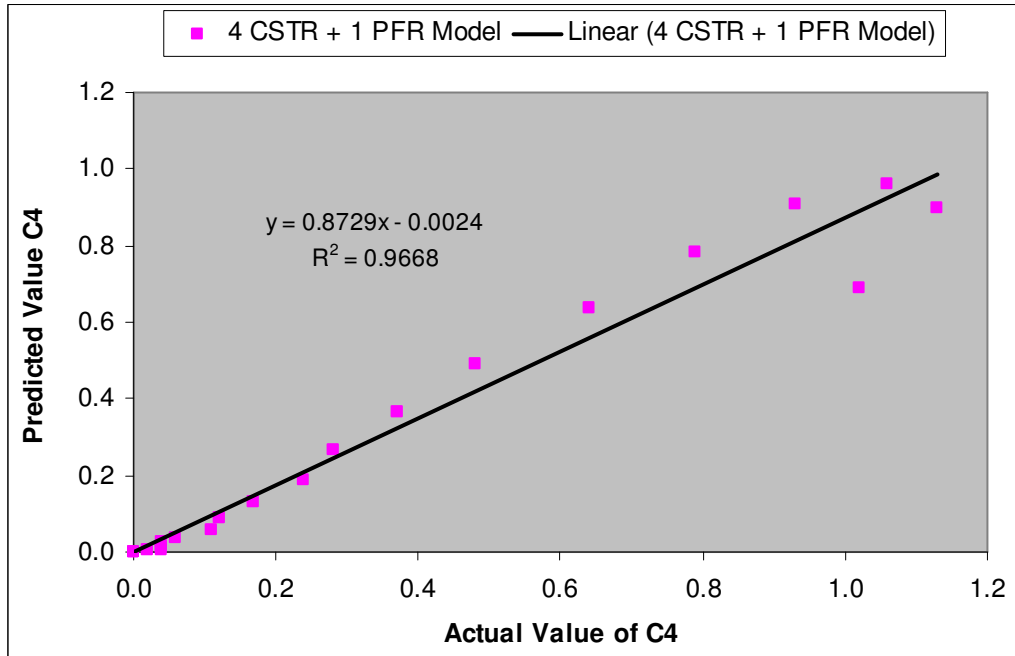
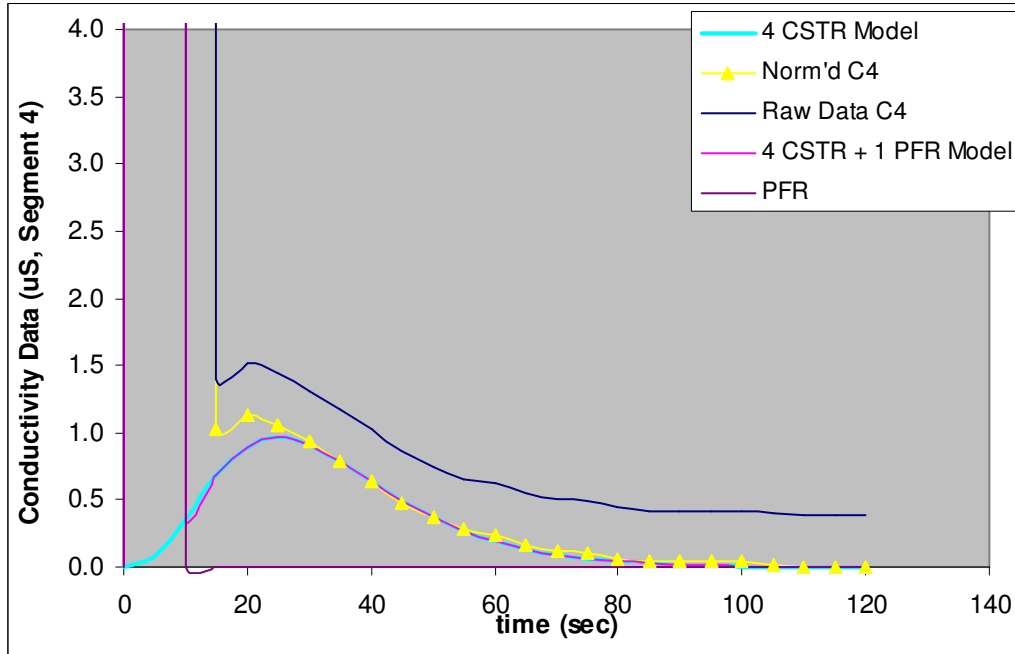


Finally, the 10.7 degree and 3.3 lpm flow: three very high conductivities (>900 μS vs. range of 0 to 1.2) were observed early in the outlet flow, between 0 and 15 seconds.

They were qualitatively consistent with the proposed model of a PFR in parallel with the

four CSTRs in series; however, the values were quite large and the model was unable to predict this behavior for the given conditions. Given that this anomaly was observed at the most extreme conditions, steepest angle of inclination and highest flow rate, the model's validity should not be extrapolated beyond the ranges that were studied unless some additional data are collected to provide the user with confidence. Figure 2.12 shows the data details for this trial.

Figure 2.12: Observed outlet conductivity. (segment 4, 10.7 deg, 3.3 lpm). Plot of predicted vs. actual has eliminated the first 3 data points.



During the hydraulic investigation of the vortex generating flume, it was found that the maximum for the fitted residence time of a single CSTR ($\tau = 68$ s) occurred at the conditions of 5.52 degrees and 1.1 lpm. The experimental maximum residence time ($\tau = 39$ s) based on values determined for Q and V_{segment} was at the conditions of 4.36 degrees and

1.1 lpm, the lowest angle of inclination and flow rate. Additionally, the steepest angle of inclination and highest flow rate yielded the lowest residence times. The maximum residence time will yield the highest conversion from soluble phosphates to precipitated phosphates, provided adequate mixing can be maintained. Figure 2.13 and 2.14 below, show the fitted values for residence time for the four CSTRs in series and the PFR. In nearly all cases, except for 4.36 degrees and 2.24 lpm, the values monotonically decline as flow increases. This trend is not observed for the 4.36 degree conditions and is likely within the experimental error. Additional data collection would be needed to resolve this anomaly.

Figure 2.13: Fitted values for residence time (τ) for CSTRs and PFR for the 5 parameter model.

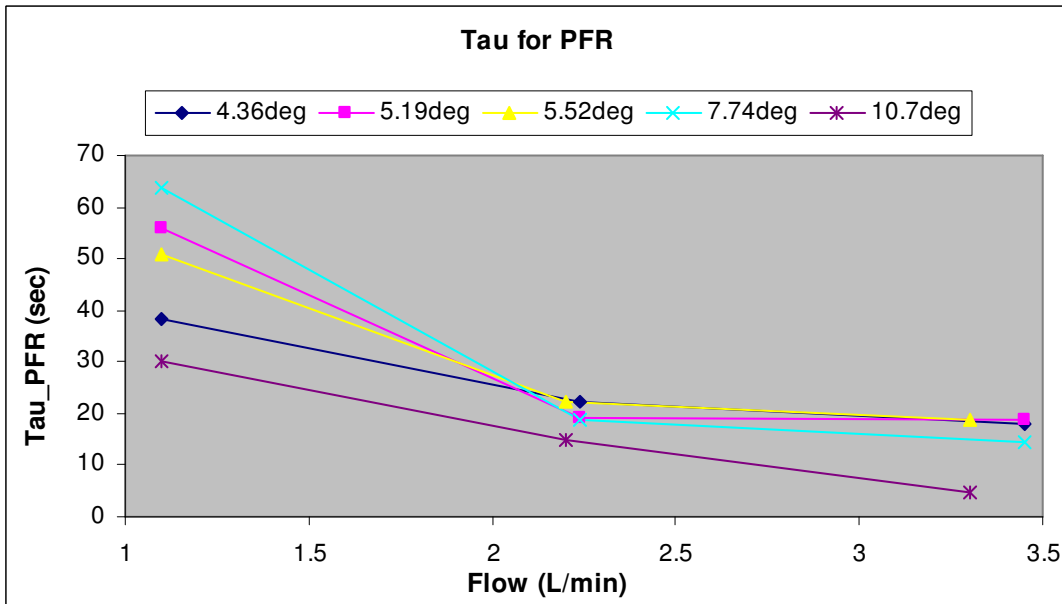
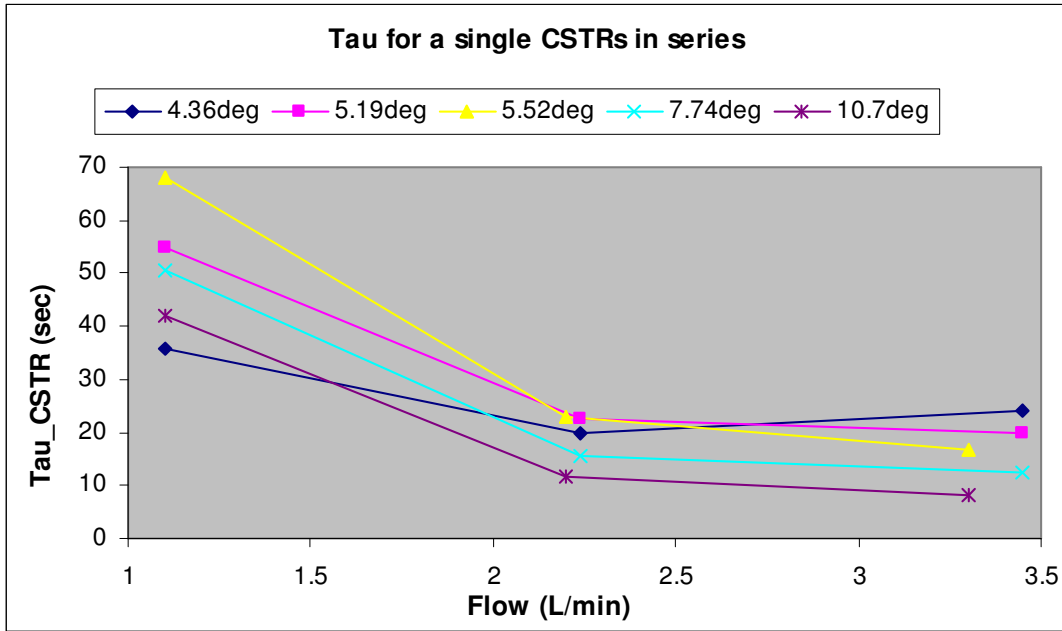
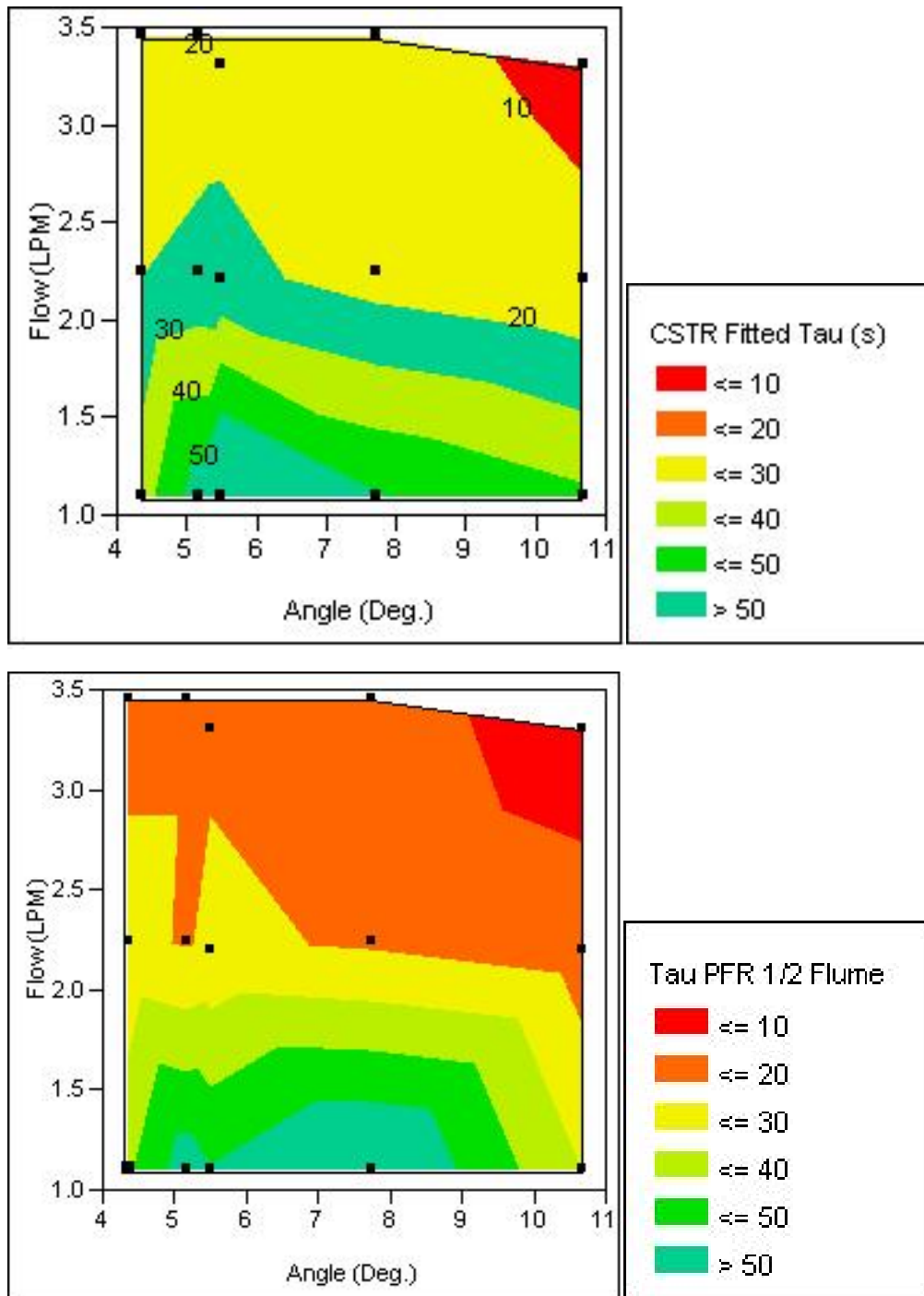


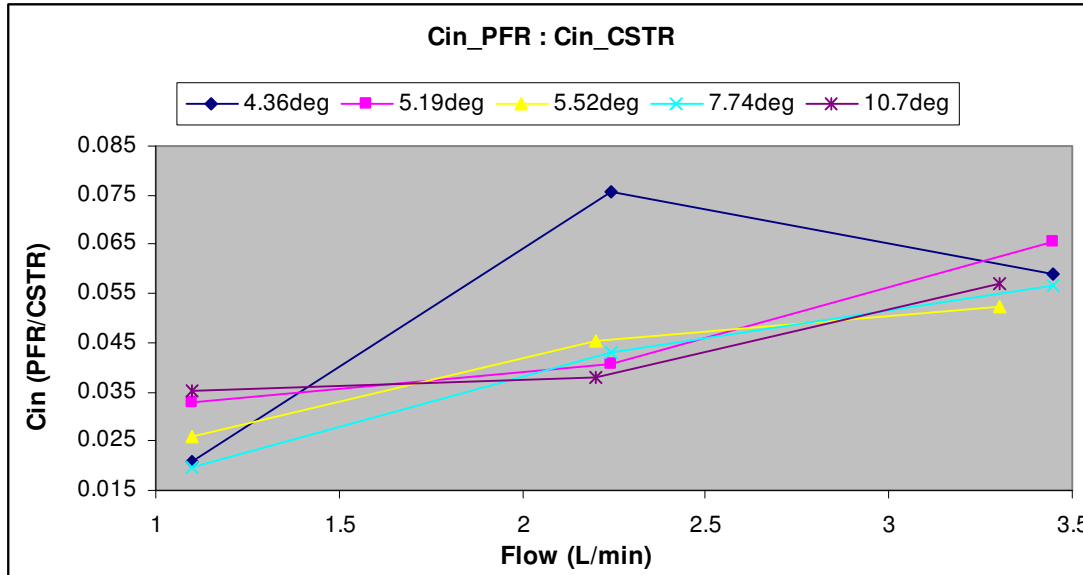
Figure 2.14: Contour plots of residence time for a single CSTR (in series of 4) and the PFR.



Examining the ratio of inlet concentrations for the PFR compared to the four CSTRs, it is apparent that in nearly all cases, except the lowest angle of inclination, that the ratio monotonically increases for increasing flow rate. This suggests that the bypass character of the system increases with flow rate. This is consistent with the observation,

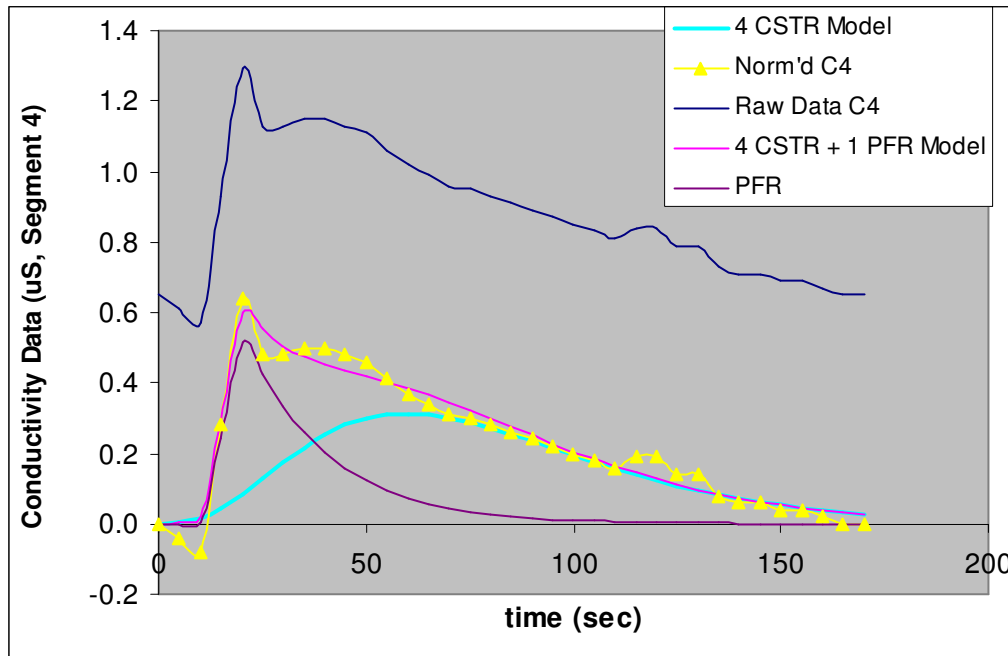
using a pulse injection of dye, that some portion appears to exit the reactor earlier. The 4.36 degrees and 2.24 lpm flow is the only data point that appears to not follow this trend. Figure 2.15 below graphically shows this trend.

Figure 2.15: Ratio of model fitted inlet concentrations of PFR to CSTR versus flow rate by angle of inclination.



The fit of the model to the data for 2.24 lpm and 4.36 degrees is very good, $r^2=0.967$, for the parameters calculated at this setting. This condition is unusual in that the fitted value for tau is less than the fitted value for the same angle and flow rate of 3.45 lpm. The data point is likely an anomaly and additional data should be collected at each condition to obtain a better estimate of the error in fitting the model. Secondly, it is observed for this data point that the baseline conductivity does not appear stable before data collection began. Figure 2.16 below shows the data set for this condition.

Figure 2.16: Observed outlet conductivity. (segment 4, 4.36 deg, 2.24 lpm).



A source of the error for this flow condition is the unstable baseline before the data collection was performed. This could also affect the values that are fit to the model and possibly explain why this particular trial appears to not fit into the general trends seen in the ratio of $C_{in_PFR}:C_{in_CSTR}$ versus flow and angle as well as the odd intermediate value for τ_{CSTR} . Additional data should be collected when there is a steady baseline to ensure that this accounts for the unexpected behavior.

Discussion and Conclusions

The overall fit of the model to the data was considerably enhanced by modifying the model from four CSTRs in series to four CSTRs in series plus a PFR in parallel. The consistent observation of a high concentration spike early in the outlet trace for all flow rates above 1.1 lpm provides confidence that the model has a physical basis. In addition, the observed behavior of the dye tracer further supports the physical basis of this model. Naturally, the fit is improved by increasing the number of parameters used to fit the model from three to five. r^2 -adj was determined to ensure the value of r^2 was not being inflated by using a five parameter versus three parameter model. The values of r^2 -adj were also found to significantly increase between the three to five parameter models. For the range of this investigation, 1.1 to 3.45 lpm and 4.36 to 10.7 degrees, the model could adequately

describe the flow behavior based on the data collected. However, some field applications may require a smaller angle of inclination. While the model could be used to extrapolate to the conditions of interest (angles less than 4.36 degrees based on physical constraints at some locations), more data would need to be collected to ensure the validity of the model in this new operating regime.

In all data sets for the adjusted model, it was observed that the fitted values for the residence time for the four CSTRs in series was greater in all cases than the calculated value. This observation suggests a high level of flow retention in the flume due to the vortices. The data were consistent such that for a given angle of inclination, as the flow rate increased, the residence time decreased for both the four CSTRs in series and the PFR. Overall, the injection times for both the PFR and CSTR could be adequately modeled by setting them to 1 second. This time is somewhat variable from run to run, but is of realistic magnitude. The only exception was for the highest flow and angle (3.3 lpm and 10.7 degrees). The initial spike in conductivity was so great that the injection time was modeled as 0.1 seconds to provide the best fit. For this particular data set, a 5 second time interval was probably too large for the low residence time and may result in missing some of the behavior observed under this condition. If additional studies pursue flow conditions near this regime, more frequent measurements will need to be made. However, for the majority of this study, 5 second intervals provided adequate data to model the flow.

The maximum residence time of 68 seconds was observed at 5.52 degrees and 1.1 lpm. Although the maximum residence time was not observed at the lowest angle of inclination and flow rate as expected, it was observed that the lowest angle of 4.36 degrees and lowest flow rates of 1.1 to 2.2 lpm provided the best agreement between calculated residence time and the best-fit residence time. As the angle of inclination and flow rates were increased, the CSTRs in parallel with a PFR model began to provide excessively larger values for the residence time versus the calculated values. This observation is in line with the increasing effects of the PFR flow regime at higher flow rates and steeper angles as well as having more energetic vortices at these conditions.

From a reaction kinetics standpoint, the highest residence time is the most desirable condition since it provides the longest mixing time for the reaction to occur. A practical

tradeoff will be balancing a residence time that supports a high conversion and still providing a sufficient flow that will not immediately clog the flume with particulate matter either from the waste stream or from the precipitation reaction of the soluble phosphates. The kinetics and conversion of soluble phosphates will be discussed in a later section and we will also revisit the topic of the build up of particulate matter in the flume itself.

The through-put capacity of the flume results from a compromise with the residence time. Higher flow conditions will yield greater throughput, but will yield poorer results for precipitating phosphates due to the decreased mixing and residence time. For the flows studied, Table 2.4 provides some capacity values.

Table 2.4: Volumetric capacity for phosphate precipitating flume.

# of Flumes	Flow Rate (lpm)	Flow Rate (gal / 24hr day)
1	1.1	418
1	2.24	852
1	3.45	1313
2	1.1	837
2	2.24	1704
2	3.45	2625
3	1.1	1255
3	2.24	2557
3	3.45	3938

For even low flows of 1.1 lpm, capacity can be relatively high over a 24 hour period since the flume operates under gravity flow. A single flume of the tested pilot scale can process approximately 418 gallons of liquid waste per day up to 1313 gallons per day for a flow rate of 3.45 lpm. For larger animal production facilities, the capacity is fully scalable based on the number of flumes installed and their physical scale.

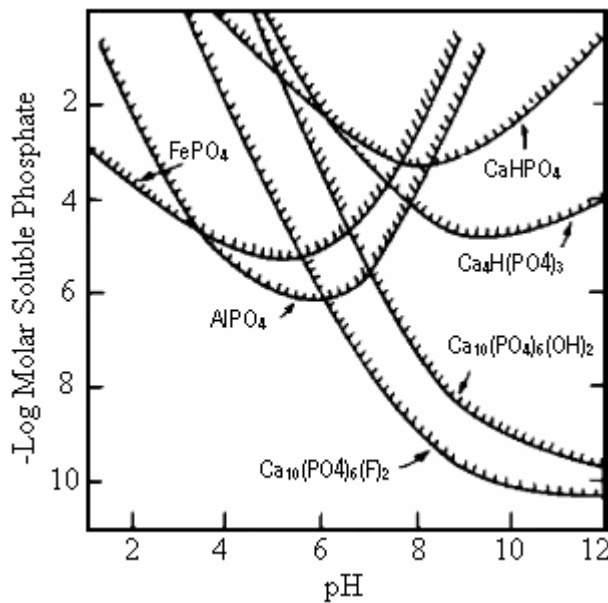
In conclusion, the operation of the vortex generating flume is well modeled by using the four CSTRs in series with a smaller PFR in parallel. Fitted values for residence times were found to be in the range of 8 to 68 seconds depending on the operating conditions. This range should provide an adequate residence time to support a high conversion of soluble to insoluble phosphates. The waste capacity of the flume is fully scalable to meet the throughput needs of any animal or agricultural production facility under normal conditions. Additional work will be needed if the flume is to be operated outside of the operating window investigated and such work could enhance the model by providing further data for better estimating the error.

CHAPTER 3 - KINETIC MODEL

Introduction

Phosphates can be precipitated by a variety of methods. Common methods include precipitation with metallic salts containing iron, calcium, or aluminum. These particular treatments can be tailored to a specific region or soil type in order to avoid having to adjust pH to facilitate precipitation. Figure 3.1 below, adapted from Stumm and Morgan (1981) shows the effects of pH on soluble phosphates.

Figure 3.1: Solubility of metal phosphates (Stumm and Morgan, 1981).

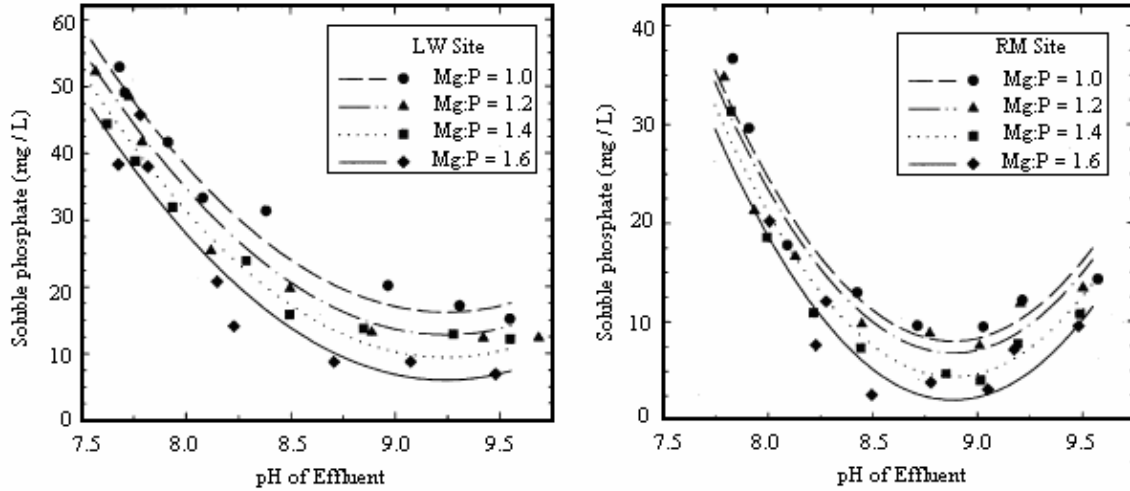


Another common way to precipitate phosphates is by the addition of magnesium, typically in the form of MgCl₂ to waste streams to yield struvite, MgNH₄PO₄·6H₂O. Struvite is an attractive option from the standpoint it has a dual purpose. Not only does precipitation of struvite remove ammonium and phosphates from waste lagoons, the mineral precipitate itself can be used as a controlled, time released fertilizer (Bridger et al, 1962). This is attractive both environmentally and economically. The solubility of these precipitates, similar to those from Figure 3.1, can largely depend on the ambient pH and the molar ratio of the metallic concentration to the phosphate concentration.

Nelson et al (2003) found that for swine lagoons, the optimum conditions for precipitating struvite was a pH range of 8.9 to 9.25 depending on the location of the swine lagoon and the ambient conditions. Furthermore, it was found that the molar ratio of Mg to

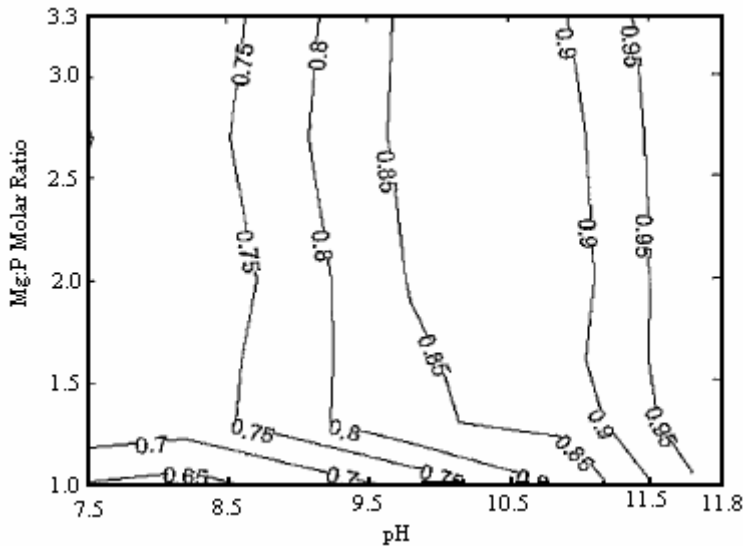
P affected the concentration of soluble phosphates (Nelson et al, 2003 and Beal et al, 1999). A value of 1.6:1 (Mg:P) was determined to best precipitate the phosphates. Figure 3.2 below, adapted from Nelson et al (2003) shows these data graphically.

Figure 3.2: Dissolved phosphate concentrations in anaerobic swine lagoons. LW and RM are swine lagoon locations in North Carolina. (Nelson et al, 2003).



Additionally, Yang et al (2006) reports that the solubility product for precipitation by magnesium is $K = 2.5 \times 10^{-12}$ in studying phosphate precipitation to struvite in mixed wastewater. The research also indicated that the maximum percentage of phosphates removed was observed at pH values of 11.8. The molar ratios were also varied for Mg:P from 1.0 up to 3.3. It was found that increasing the molar ratio of Mg:P above 1.3 yielded little to no improvement in the precipitation. Figure 3.3 below, adapted from Yang et al (2006) provides a contour plot of phosphorus removal versus Mg:P molar ratio and pH. As shown, the total phosphorus removal is highly dependent on pH.

Figure 3.3: Affects of Mg:P (from MgCl₂) and pH on the percentage of phosphates removed from mixed waste water streams. Inlet phosphate concentration ranged from 0.50 to 1.77 mg/L. (Yang et al, 2006).



In addition, there are software packages such as USEPA's Minteqa2, a Windows based program developed by the US EPA, which can model a wide array of conditions and multiple phase reactions. Additional software such as DESASS or Activated Sludge Models, ASM2,3,4, have also been used model phosphate precipitation (Ferrer et al, 2007). Of the numerous methods to precipitate phosphates, this paper will focus on precipitation with magnesium to form struvite.

Methodology

The reaction kinetic data collected by Nelson et al (2003) from a swine lagoon were incorporated into the hydraulic model of the flume discussed earlier. The same Excel files were modified to determine the mean conversions using the model parameters and the kinetic data from Nelson et al (2003). Nelson determined three values for the rate constant depending on the pH. Values ranged from 3.7 h⁻¹ at a pH of 8.4 to 12.3 h⁻¹ at a pH of 9.0. This range of values was evaluated to provide lower and upper bounds for the percentage of phosphates that could be effectively removed using the vortex generating flume. In addition, a wide range of phosphate concentrations were considered, ranging from 63 mg/L up to 540 mg/L (Nelson et al, 2003 and Celen and Buchanan et al, 2007). Heat of reaction effects were ignored in this study based on the large thermal mass of the waste stream and

the exposure to ambient conditions. US EPA (1986) and Yang et al (2006) indicate that a common goal in total phosphorus removal is the threshold value of <0.05mg/L in the effluent of a treatment system. This value will be the target metric for evaluating the optimum conditions for the vortex generating flume.

Kinetic Model

According to Nelson et al (2003), phosphate precipitation via struvite can be adequately modeled using first order, irreversible kinetics. Equation 5 and 6 provide the chemical reaction and the rate law for the reaction (Metcalf and Eddy, 2003):



and

$$-r_{\text{PO}_4^{3-}} = k \cdot C_{\text{PO}_4^{3-}} \quad (6)$$

(Nelson et al) in which $-r_{\text{PO}_4^{3-}}$ is the rate of disappearance of soluble phosphates, k is the reaction rate constant, and $C_{\text{PO}_4^{3-}}$ is the concentration of soluble phosphates. The mean conversion, \bar{X} for a first order reaction is given by:

$$\bar{X} = \frac{\tau \cdot k}{1 + \tau \cdot k} \quad (7)$$

The tau used in the model is the same as the value determined for the mean residence time for each condition investigated in the hydraulic model. The conversion is then determined for each CSTR in the model. The overall conversion of the system is determined from the amount of phosphate precipitated versus the overall initial amount of soluble phosphates. The kinetics are adequately described as first order and irreversible for the given conditions; it is noted that the conversion is independent of the initial phosphate concentration. Thereby, we expect to see the same conversion in the model regardless of initial concentration. The main difference in operating conditions is then dependent on the inlet concentration, as it will dictate the outlet concentration in the effluent stream. Alternatively, the reaction could be modeled as a reversible reaction as in Celen and Buchanan et al (2007) and Yang et al (2006). Advantages to modeling the struvite precipitation in this manner are that it accounts for the effects of pH on the solubility of the species formed and can be used to predict over a wider range of

operating conditions. The main focus of this paper will be on using simple first order kinetics.

The operating conditions of the flume also change in that instead of the pulse tracer used to characterize the flow, the feed will be a step input of concentration from the subsequent waste stream.

Results

Various inlet concentrations of phosphates were tested in the model. Values ranged between 63.8 and 540 mg/L, as found in the literature (Nelson et. al, 2003 and Celen and Buchanan et al, 2007). Table 3.1 shows the predicted mean conversions for all given flow conditions over the range of the rate constant for several initial phosphate concentrations. The range in values for the rate constants were estimated from studies by Nelson et al (2003) and further supported by values reported by Ohlinger et al (2000).

Table 3.1: Conversion of soluble phosphates to precipitated phosphates for Cinlet = 63.8mg/L.

Angle (Deg.)	Flow (LPM)	CSTR Inlet (PO ₄) ³⁻ (mg/L)	PFR Inlet (PO ₄) ³⁻ (mg/L)	CSTR		PFR		System		System	
				k=3.7h ⁻¹ (PO ₄) ³⁻ Outlet (mg/s)	k=12.3h ⁻¹ (PO ₄) ³⁻ Outlet (mg/s)	k=3.7h ⁻¹ (PO ₄) ³⁻ Outlet (mg/s)	k=12.3h ⁻¹ (PO ₄) ³⁻ Outlet (mg/s)	k=3.7h ⁻¹ (PO ₄) ³⁻ Outlet (mg/L)	k=12.3h ⁻¹ (PO ₄) ³⁻ Outlet (mg/L)	X for k=3.7h ⁻¹	X for k=12.3h ⁻¹
4.36	1.1	63.8	1.3	1.63E-03	2.39E-05	4.34E-04	3.09E-04	0.112	0.018	99.82%	99.97%
4.36	2.24	63.8	4.8	4.06E-02	1.09E-03	1.24E-02	1.01E-02	1.419	0.301	97.78%	99.53%
4.36	3.45	63.8	3.8	3.16E-13	2.59E-15	1.18E-02	1.00E-02	0.206	0.174	99.68%	99.73%
5.19	1.1	63.8	2.1	9.26E-16	7.58E-18	1.00E-03	6.23E-04	0.055	0.034	99.91%	99.95%
5.19	2.24	63.8	2.6	3.48E-14	2.85E-16	3.68E-03	3.08E-03	0.098	0.083	99.85%	99.87%
5.19	3.45	63.8	4.2	3.68E-13	3.02E-15	1.46E-02	1.23E-02	0.254	0.214	99.60%	99.66%
5.52	1.1	63.8	1.7	2.69E-16	2.20E-18	6.48E-04	4.18E-04	0.035	0.023	99.94%	99.96%
5.52	2.2	63.8	2.9	1.00E-13	8.22E-16	4.39E-03	3.59E-03	0.120	0.098	99.81%	99.85%
5.52	3.3	63.8	3.3	4.01E-13	3.29E-15	8.95E-03	7.55E-03	0.163	0.137	99.74%	99.78%
7.74	1.1	63.8	1.3	3.85E-05	3.92E-07	3.57E-04	2.09E-04	0.022	0.011	99.97%	99.98%
7.74	2.24	63.8	2.8	8.87E-03	1.57E-04	4.11E-03	3.46E-03	0.348	0.097	99.46%	99.85%
7.74	3.45	63.8	3.6	3.45E-13	2.83E-15	1.10E-02	9.65E-03	0.192	0.168	99.70%	99.74%
10.7	1.1	63.8	2.3	8.75E-16	7.17E-18	1.29E-03	9.86E-04	0.070	0.054	99.89%	99.92%
10.7	2.2	63.8	2.4	4.23E-14	3.47E-16	3.17E-03	2.76E-03	0.087	0.075	99.86%	99.88%
10.7	3.3	63.8	3.6	3.33E-02	7.41E-04	1.12E-02	1.07E-02	0.809	0.209	98.73%	99.67%

Additional inlet concentrations were tested ranging from 150 to 540 mg/L and the results can be found in the Appendix. The phosphate conversion at all conditions is very high; all values are above 97%, with most above 99%. The determining factor for which operating condition will yield the best removal rate is dependent on which condition has the least amount of PFR type flow and a high value for the residence time.

Figure 3.4a and b and 3.5a and b below, are contour plots of the outlet concentrations of phosphate for the minimum and maximum rate constants found in Nelson et al (2003) at the minimum and maximum phosphate concentrations at the inlet of the flume.

Figure 3.4a: Contour plots of modeled outlet phosphate concentration for $C_{in} = 63.8\text{mg/L}$ for $k = 3.7\text{h}^{-1}$.

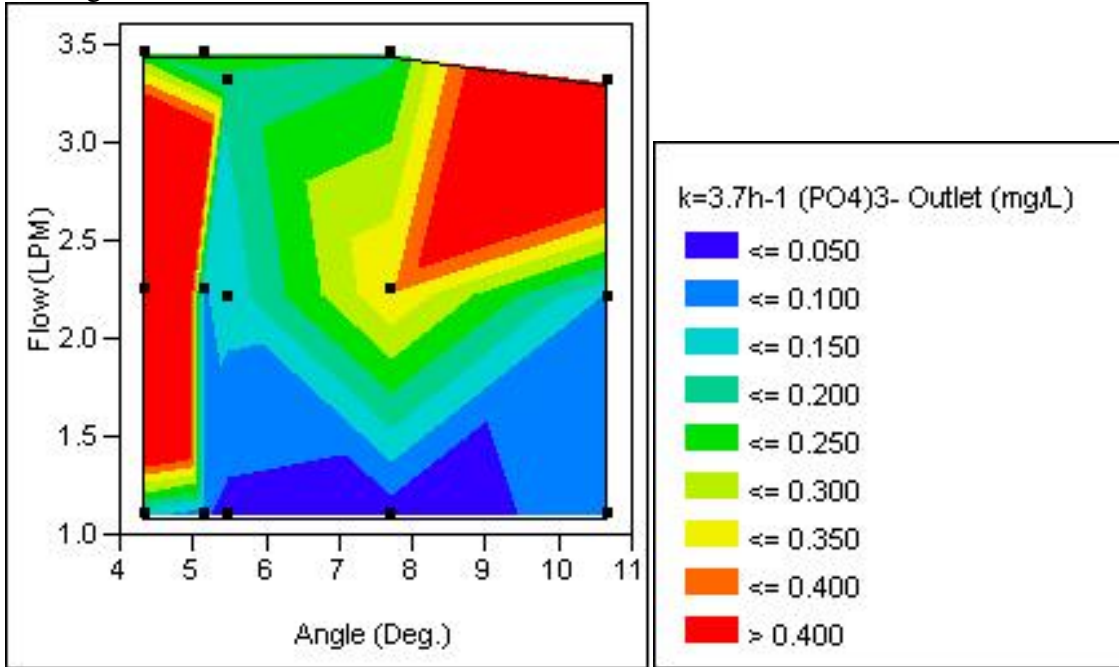


Figure 3.4b: Contour plots of modeled outlet phosphate concentration for $C_{in} = 63.8\text{mg/L}$ for $k = 12.3\text{h}^{-1}$.

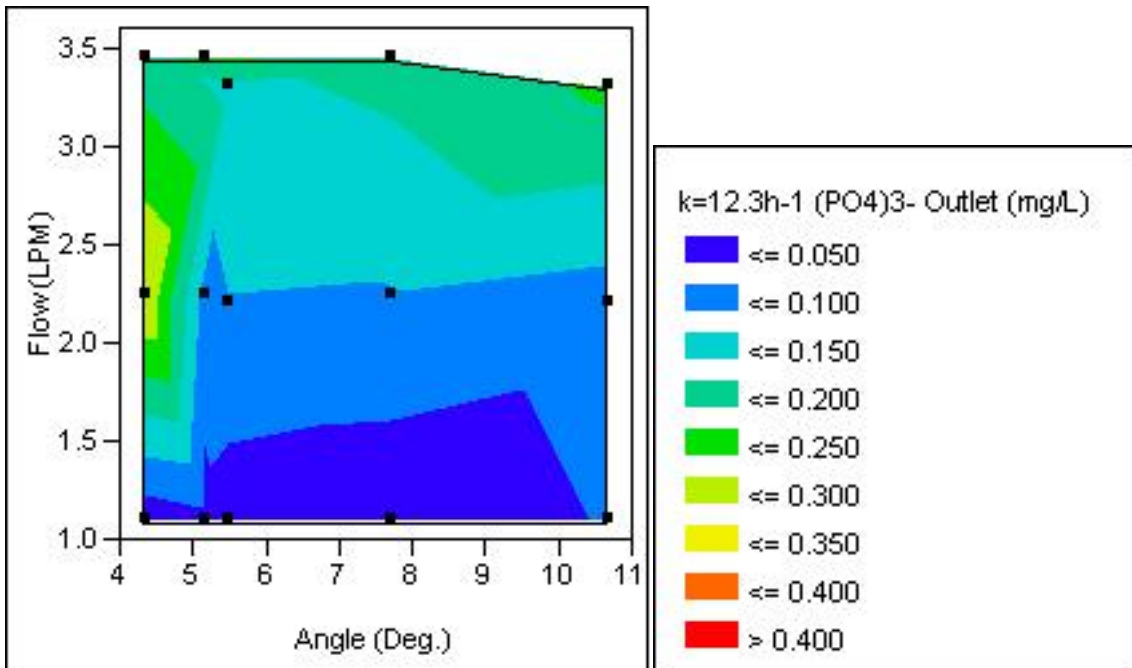


Figure 3.5a: Contour plots of modeled outlet phosphate concentration for $C_{in} = 540\text{mg/L}$ for $k = 3.7\text{h}^{-1}$.

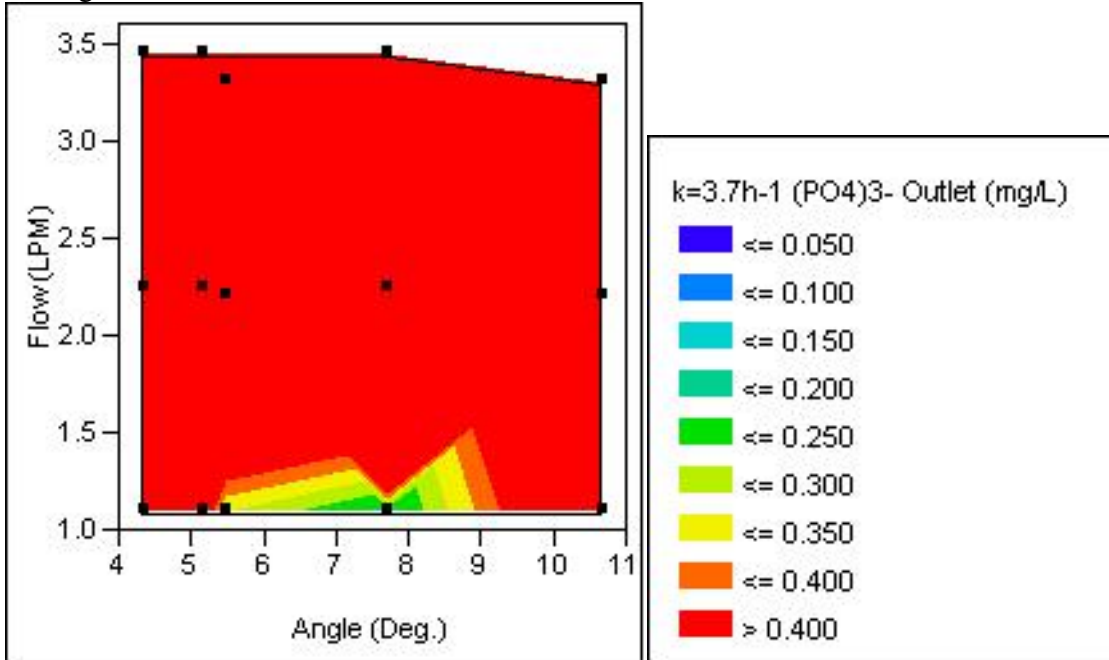
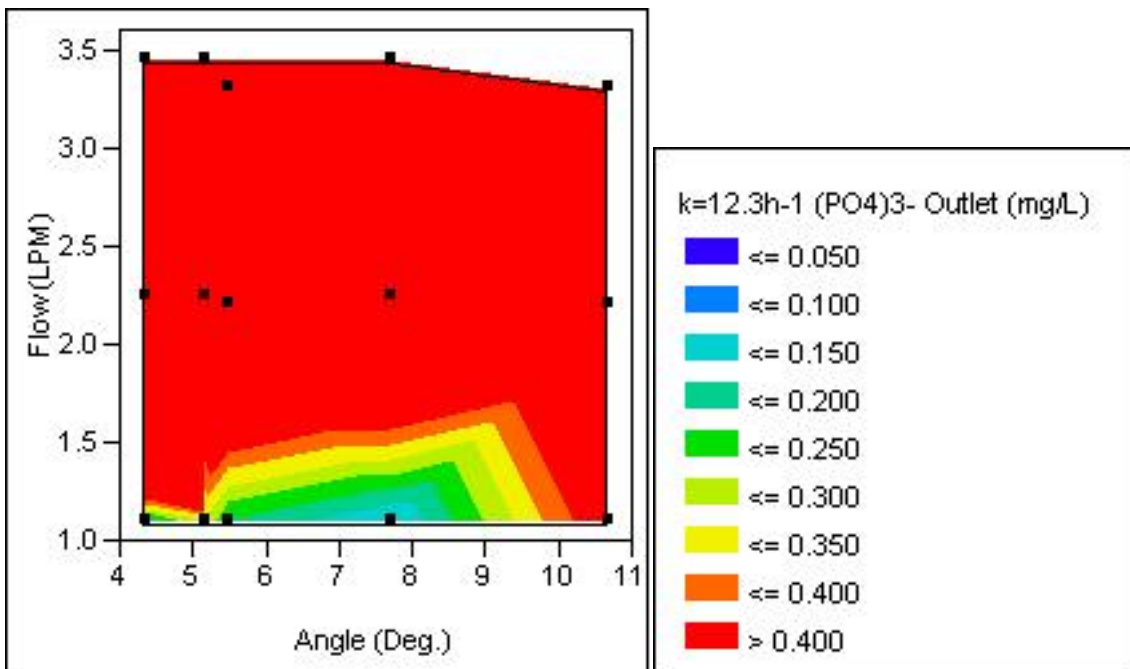


Figure 3.5b: Contour plots of modeled outlet phosphate concentration for $C_{in} = 540\text{mg/L}$ for $k = 12.3\text{h}^{-1}$.



For the lowest phosphate concentration considered in this study, 63.8 mg/L for $k=3.7\text{ h}^{-1}$, it is observed that for the lowest flow rate of 1.1 lpm the angles of inclination that yield results less than 0.05 mg/L are the intermediate angles: 5.19 , 5.52 , and 7.74 .

The highest outlet concentrations occur at the highest angle and highest flow rate, but also at the lowest angle and an intermediate flow rate, 4.36 degrees and 2.24 lpm. This condition has the highest ratio of $C_{in_PFR}:C_{in_CSTR}$, which is the case with the most predominant PFR behavior. Intuitively, the lowest residence time conditions (steep angle, high flow) are expected to have the highest outlet concentrations, but for a reaction rate constant of 3.7 h^{-1} , this is not the case. At the same inlet concentration and with $k=12.7 \text{ h}^{-1}$, all angles but the steepest, 10.7 degrees yields results less than 0.05 mg/L. An important observation is that the outlet concentration from the PFR portion of the modeled flow is either the same order of magnitude or up to many orders of magnitude greater than the four CSTRs in series contribution. This accounts for the higher than expected outlet phosphate concentrations at this condition. However, given that the 1.1 lpm and 3.45 lpm flows at the same angle do not exhibit this behavior suggests that further data collection is warranted to obtain a better estimate of error for the flume's operating space.

For the highest phosphate concentration considered in this study, 540 mg/L, it was found that none of the conditions met the criterion of $<0.05 \text{ mg/L}$ and conversion greater than 95%. However, the flow rate of 1.1 lpm and 7.74 degrees yielded the lowest concentration. This result is consistent with phosphorus levels for other inlet concentrations. Additional inlet concentrations were tested to determine an effective maximum such that the current process window would yield an effluent of 0.05 mg/L of phosphorus or less. Figure 3.6a and b below, illustrates an inlet concentration of 150 mg/L. Note that the lower value of the reaction rate constant does not yield a solution space in which the phosphorus concentration is below 0.05 mg/L, but the higher reaction rate constant does.

Figure 3.6a: Contour plots of modeled outlet phosphate concentration for $C_{in} = 150\text{mg/L}$ for $k = 3.7\text{h}^{-1}$.

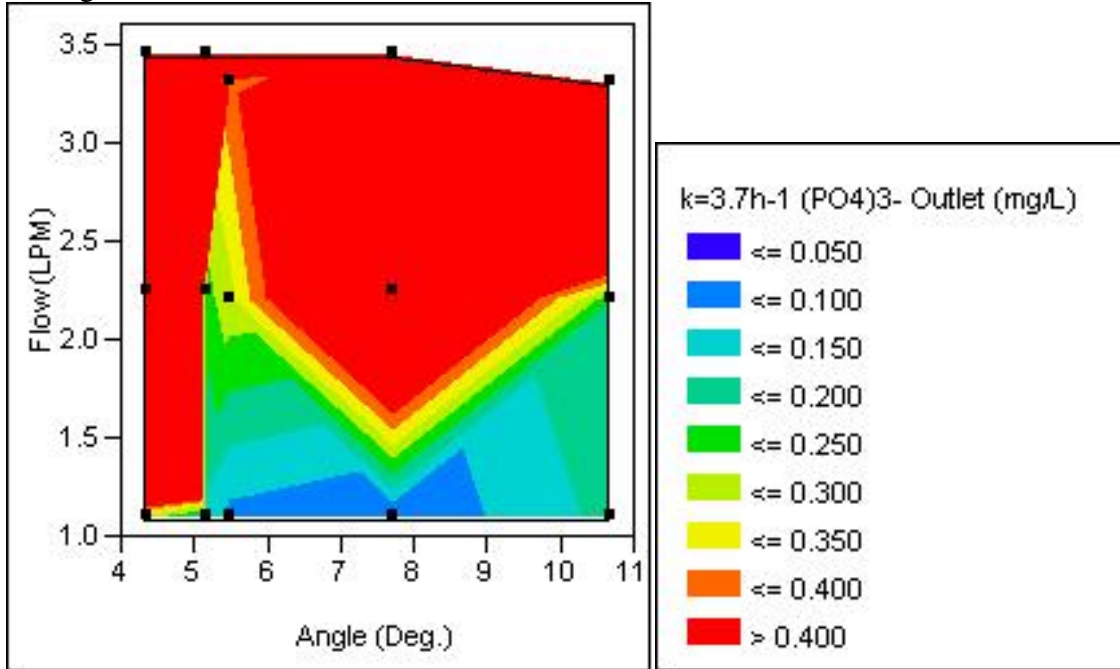
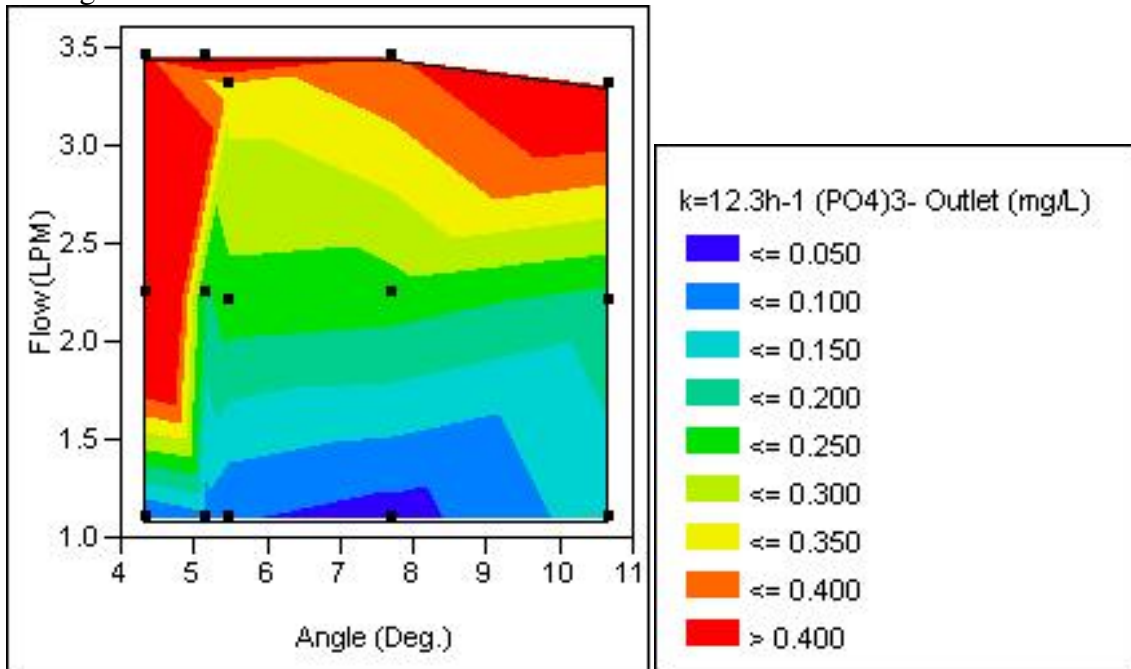


Figure 3.6b: Contour plots of modeled outlet phosphate concentration for $C_{in} = 150\text{mg/L}$ for $k = 12.3\text{h}^{-1}$.



It can be noted that at all conditions, the conversion of soluble phosphates to precipitate occurs at intermediate angles of inclination and lower flow rates. The flow rate is a much stronger modulator of outlet phosphorus concentration than angle of

inclination as observed in the contour plots. Finally, all conditions simulated provided a very high conversion, >97.7%.

Discussion and Conclusions

In this study a wide range of possible phosphate concentrations were considered, ranging from 63.8 to 540 mg/L. Rate constant values ranged from 3.7 to 12.3 h⁻¹ depending on the pH at which the reaction was carried out. For the lowest reaction rate constant of 3.7 h⁻¹ (corresponding to a near neutral pH of 8.4), two of fifteen operating conditions were able to yield effluent with a total phosphate concentration <0.05 mg/L. For a given site to have phosphate concentrations lower than 63.8 mg/L suggests that lower angle of inclination applications are feasible if a particular site does not have the necessary elevation difference. The results also suggest that unless the phosphate concentration is significantly above 63.8 mg/L, an elevation in pH might not be required and could thus reduce complexity and cost of operation.

Ambient conditions and variations in individual waste streams will need to be evaluated before implementing such a device at a particular agricultural or industrial site. Variations in temperature, pH of the waste streams, pH of the cropland, quantity and concentration of the waste stream, and possible angles that can be utilized to balance low phosphate concentration in the effluent and still achieve a sufficient capacity to meet peak production levels, will need to be accounted for.

Future work should include investigating other methods by which phosphate could be precipitated. Other common methods utilize calcium, aluminum, or iron. Again, chemical choice could be customized depending on ambient conditions such as runoff pH (affected by the type of soil) or the pH of a waste stream depending on the types of animals producing it. Overall selection is dependent on the method that meets the effluent requirements and is the least expensive. A second aspect of future investigation would be to quantify the effects of temperature on the reaction rate constant. Temperature swings of greater than 60 degrees are quite common in the United States. Given that most reaction rates approximately double, or halve, for a given temperature swing of 10 degrees, flume operating conditions may need to be adjusted between summer and winter seasons. A final matter of practicality is that the chosen operating

condition needs to be somewhat robust to account for accumulation of particulate matter. Higher flow rates and steeper angles likely minimize the amount of build up in the flume, but additional investigations of scour are required and the importance will likely depend on the type of waste stream that is being processed in the flume.

Additional modeling could also utilize software such as MINTEQA2 from the USEPA (Celen and Buchanan, 2007) or DESASS (Ferrer et al, 2007), which has been accurately used in many studies to compare models to collected data. These applications could greatly simplify an investigation of the entire range of conditions under which the flume may be operated.

CHAPTER 4 - CONCLUSIONS AND FUTURE WORK

Initially, the vortex generating flume was modeled as four CSTRs in series given the four distinct mixing regions separated by weirs. The model was suitable and provided good agreement with the data for the lowest flow rate (1.1 lpm). The parameters of residence time, initial concentration of electrolyte pulse tracer, and the injection time were used to fit the model. The sum of squares error between the predicted versus actual data was minimized using Excel for the outlet of the flume.

The model was improved at higher flow rates by considering the flume to have a mixture of flow types, the main component was still modeled at four CSTRs and an additional PFR was added in parallel. It has been shown that the residence time distribution of the vortex generating flume can be adequately modeled by using four CSTRs in series with a PFR operating in parallel. The PFR was modeled as a series of sixty tanks in series in order to simulate plug flow. The basis for this physical model stems from observing both the dye tracer and the experimental data measuring conductivity for a pulse electrolyte tracer. Both observations suggested a form of channeling in which some volume of higher concentration flow bypasses the vortex generating regions, escapes over the weirs without being well mixed, and exits the flume earlier than the bulk flow. Visual observation of the dye tracer validated this change. In addition, data sets with flow rates greater than 1.1 lpm also showed a characteristic spike in conductivity early in the measurements for the last weir on the flume. This more advanced model fit the data better than the simpler four tanks in series model.

A total of five parameters were used to fit the data, and r^2 -adj was also determined to ensure the fit of the model was not being inflated by using five parameters. The r^2 value for ten of the fifteen operating conditions were greater than 0.95. Of the remaining five operating conditions in which r^2 was less than 0.95, three of these conditions were strongly skewed by outliers in the data sets. With these values filtered, r^2 was greater than 0.95.

The outliers observed for these conditions have several explanations: plug flow of low conductivity solution after the initial electrolyte pulse tracer, unstable baseline of conductivity between trials, or errors in conducting the experiment. Of the remaining

two operating conditions, r^2 was greater than 0.85. Trends in the data suggest that as flow rate increases, the bypass flow over the weirs will increase and could substantially affect the outlet concentration of phosphorus due to the relatively small residence time. The residence time for the portion of the flume modeled by four CSTRs ranged from 3.2 to 6.8 times greater than the PFR residence times. The flow rate was the dominant factor affecting residence times in the flume; the angle of inclination had only a minor impact over the ranges studied. The fit of the model was consistent with the physical operation of the flume in that the bulk of the flow appeared to be well mixed in the four CSTRs while only a smaller portion of the flow bypassed the mixing regions generated by the weirs.

The application of first order, irreversible kinetics to precipitate phosphorus with magnesium chloride was added to the model using the same reactor configuration. The conversion was independent of inlet concentration since the kinetic model was first order, depending only on the reaction rate constant and the residence time. The conversions in all cases were >97% and suggest that the vortex generating flume can provide an adequate and feasible solution to preventing nutrient enrichment of waterways due to feedlot or agricultural runoff. Furthermore, precipitation using $MgCl_2$ to yield struvite is an attractive solution since it also results in decreasing NH_4^+ in the waste stream as well. The simultaneous reduction of both phosphorus and nitrogen in the waste effluent reduces the effects of downstream nutrient enrichment. In addition to the co-precipitation of these two nutrients, the mineral struvite itself is of value as a time-released fertilizer (Bridger et al, 1962). Collection of the precipitate can be used in nutrient deficient areas or sold off-farm to offset the costs of a nutrient management plan.

A potential disadvantage is that if the molar ratio of the waste stream for N:P is insufficient, an alternative method may need to be investigated for phosphorus removal. Other options would include using Ca, Fe, or Al. A fourth option, MgO is attractive since it will precipitate the phosphorus as struvite and also increase the removal efficiency due to the elevation in pH. Multiple studies have shown that the solubility of phosphorus precipitates is highly dependent on pH. Depending on the surrounding environment and soil type, using one metallic salt over the other may be advantageous, but will also need to be balanced with cost differences.

The preliminary data suggest that vortex generating flumes can provide a practical and cost effective method for removing phosphates from animal and agricultural production facilities. Depending on the conditions at the individual site: phosphate concentration, pH, temperature, and suspended solids in waste stream, some adjustments to the operation of the flume may be required. Adjustments to the pH of the waste stream may prove to be more costly depending on the region or type of waste. An alternative is to utilize one of the other metallic salts to precipitate the phosphates that have a lower solubility at ambient pH levels. Though many animal production facilities rely upon gravity-driven flow to carry waste run-off to lagoons, specific sites may not have the desired elevation difference for the flume to operate under such conditions. Additional flow modeling will be required to ensure the flume can adequately remove phosphates. In addition, most waste streams are high in particulate matter, along with the precipitation of struvite in the flume. Because of this, the minimum required scour velocity will need to be investigated. Intuitively, clogging the flume can likely be minimized by operating at higher flow rates and steeper angles of inclination. Additional options would include a settling pond or a very coarse pre-filter before the waste is introduced to the flume.

Cost is an important matter in the successful adoption of phosphate mitigation. The vortex generating flume operates under gravity flow; the initial purchase or building cost and any maintenance costs for cleaning or chemical adjustments will be the primary expenses. This is offset by the relative ease of operation and avoidance of electricity costs if a pump were to be added to the system. A particular implementing site can also look to minimize the chemical costs by selecting a precipitation reaction where the smallest pH adjustment is needed (or none at all). In addition, cleaning costs and time can be minimized by optimizing the flow to reduce solids accumulation in the flume. Finally, if struvite precipitation is the chosen method, some cost may be recovered by off-farm sale of struvite as a time released N and P fertilizer (Bridger et al, 1962).

Multiple studies have shown that software such as Minteqa2 from the USEPA can be used to model site specific conditions (Nelson et al, 2003). Such modeling can be used to avoid costly analyses for specific conditions and provide the user with a starting condition that is reasonably near the optimum.

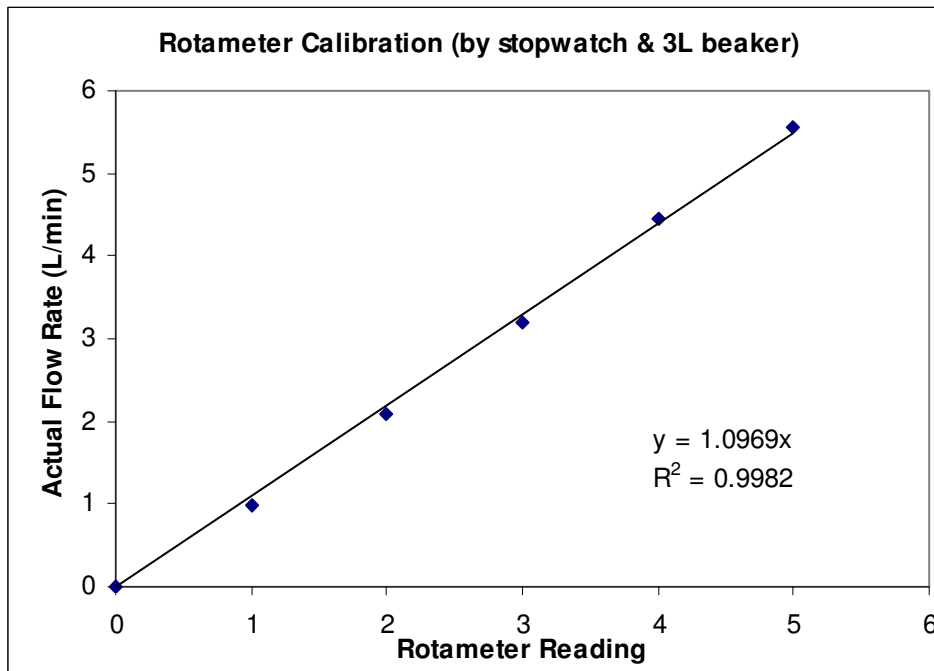
REFERENCES

- Beal, L.J., Burns, R.T., and Stadler, K.J. "Effect of anaerobic digestion on struvite production for nutrient removal from swine waste prior to land application." Presented at the 1999 ASAE Annual International Meeting. Paper No. 994042. ASAE, St. Joseph, MI.
- Bridger, G.L., Salutsky, M.L., and Starosta, R.W. "Metal ammonium phosphates as fertilizers." Journal of Agricultural Food Chemistry. 10 (1962): 181-188.
- Carpenter, S.R., Carcao, N.F., and Smith, V.H. "Nonpoint pollution of surface waters with phosphorus and nitrogen." Ecological Applications. 8 (1998): 559-568.
- Celen, I., Buchanan, J.R., Burns, R.T., Robinson, R.B., Raman, D.R. "Using a chemical equilibrium model to predict amendments required to precipitate phosphorus as struvite in liquid swine manure." Water Research. 41 (2007): 1689-1696.
- Ferrer, J., Seco, A., Serralta, J., Ribes, J., Manga, J., Asensi, E., Morenilla, J.J., and Llavador, F. "DESASS: a software tool for designing, simulating, and optimising WWTPs." Environmental Modelling and Software. (2007): 1-8.
- ILEC/Lake Biwa Research Institute, eds. Survey of the state of the world's lakes. Vols. I-IV. International Lake Environment Committee, Otsu and United Nations Environment Programme, Nairobi, 1988-1993.
- Lewandowski, J, Schauser, I., and Hupfer, M. "Long term effects of phosphorus precipitations with alum in hypereutrophic Lake Süsser See." Water Research. 37.13 (2003): 3194-3204.
- Metcalf and Eddy. Wastewater engineering: Treatment and reuse. 4th ed. McGraw-Hill, NY, 2003.
- Nelson, N.O., Mikkelsen, R.L., and Hesterberg, D.L. "Struvite precipitation in anaerobic swine lagoon liquid: effect of pH and Mg:P ratio and determination of rate constant." Bioresource Technology. 89 (2003): 229-236.
- Ohlinger, K.N., Young, T.M., and Schroeder, E.D. "Post digestion struvite precipitation using a fluidized bed reactor." Journal of Environmental Engineering. 126 (2000): 361-368.
- Reddy, K.R., Connor, G.A.O., and Gale, P.M. "Phosphorus sorption capacities of wetland soils and stream sediments impacted by dairy effluent." Journal of Environmental Quality. 27 (1998): 438-447.
- Rodhe, W. "Crystallization of eutrophication concepts in North Europe." In:

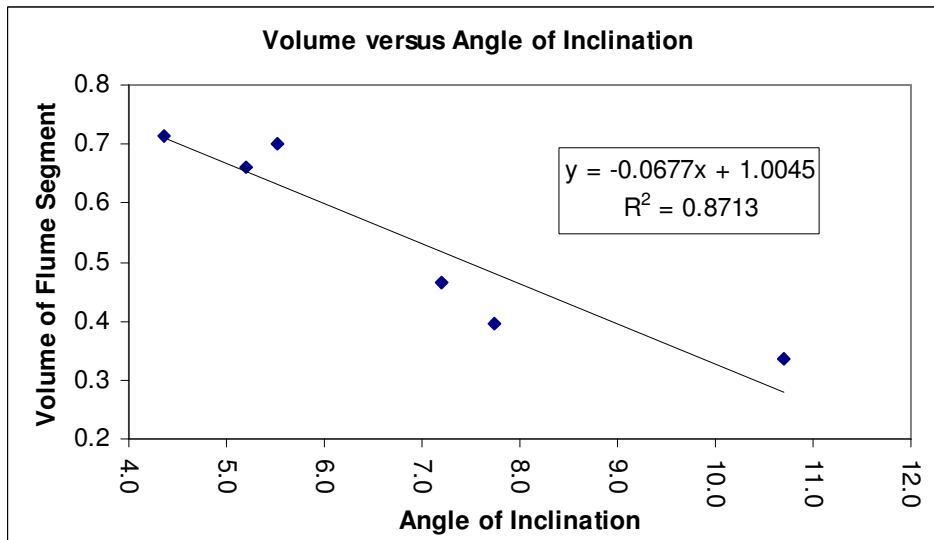
- Eutrophication, Causes, Consequences, Correctives. National Academy of Sciences, Washington, D.C., 1969: 50-64.
- Sharpley, A.N., Daniel, T., Sims, T., Lemunyon, J., Stevens, R., and Parry, R. "Agricultural phosphorus and eutrophication." US Department of Agriculture, Agricultural Research Service. ARS-149 (1999): 1-34.
- Stumm and Morgan. Aquatic chemistry: An introduction emphasizing chemical equilibria in natural waters. 2nd ed. John Wiley & Sons Inc, NY, 1981: 404-408.
- UNEP, "United Nations Environment Programme: Lakes Reservoirs vol.3, Water Quality: The Impact of Eutrophication." 2002, UNEP.
http://www.unep.or.jp/ietc/publications/short_series/lakereservoirs-3/fwd.asp
- USEPA. "National Assessment Database: Assessment Data for the State of Kansas Year 2004." 2004. USEPA.
http://iaspub.epa.gov/waters/w305b_report_control.get_report?p_state=KS
- USEPA. Quality criteria for water. Office of Water Regulation and Standards. EPA-440/5-86-001. (1986). USEPA, Washington, DC.
- Yang, L., Zhou, H., and Moccia, R. "Membrane filtration coupled with chemical precipitation to treat recirculating aquaculture system effluents." Journal of Environmental Quality. 35 (2006): 2419-2424.

APPENDIX

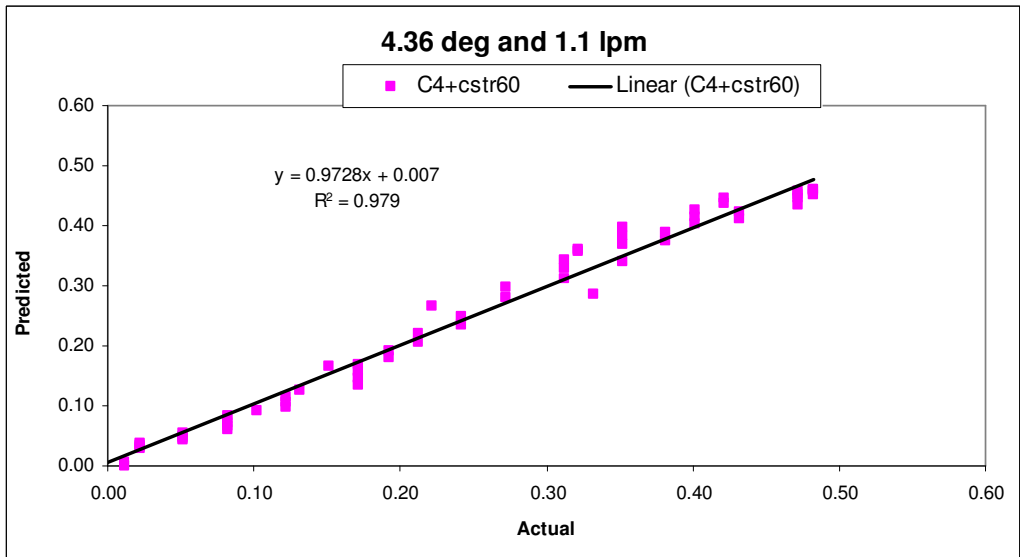
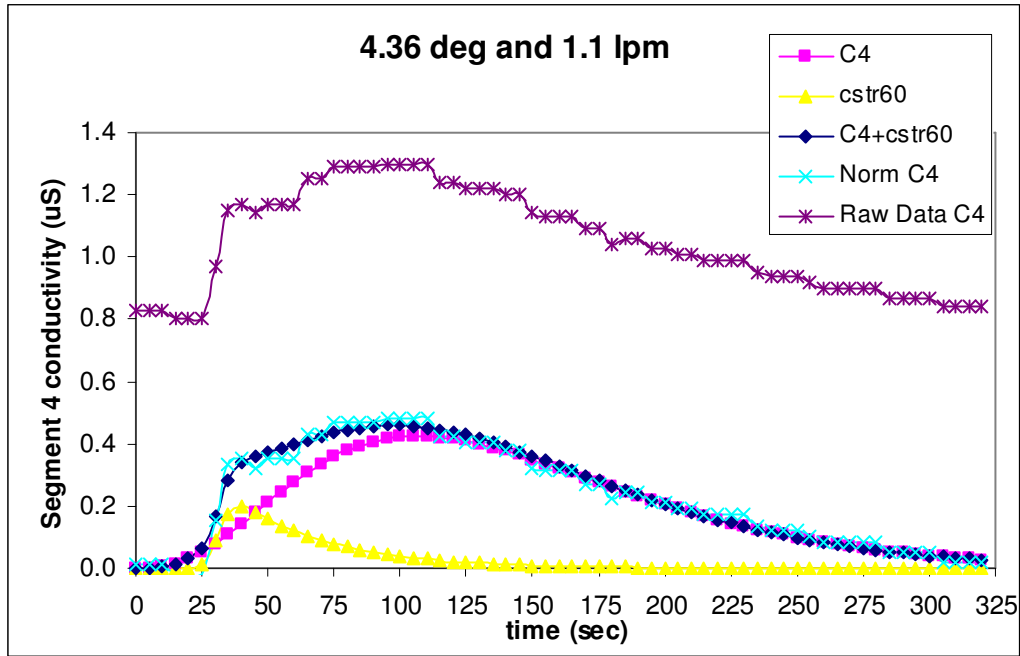
Rotameter Calibration

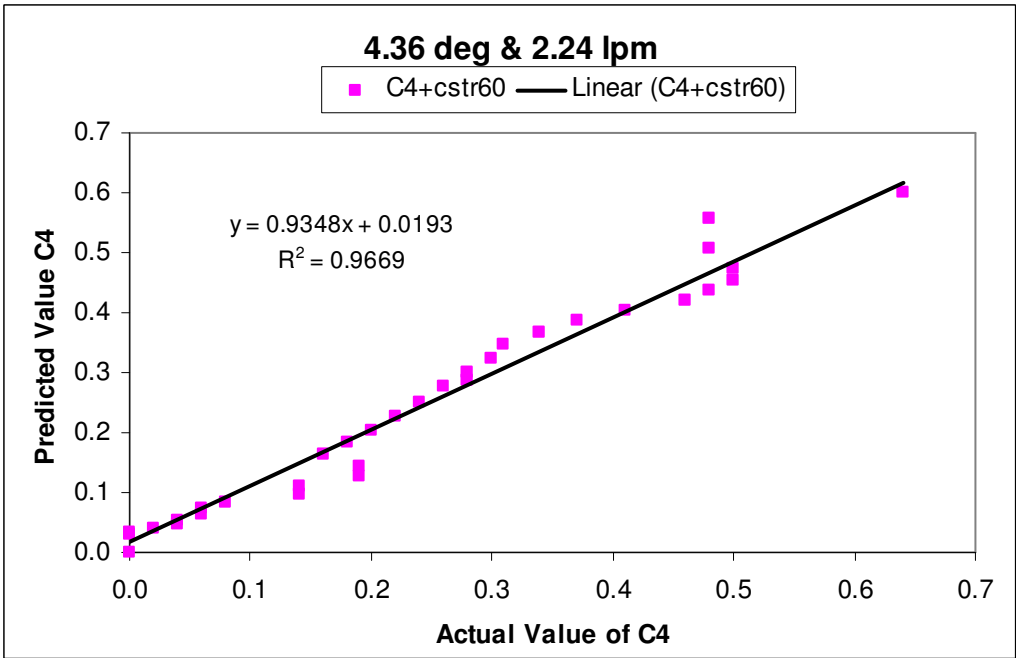
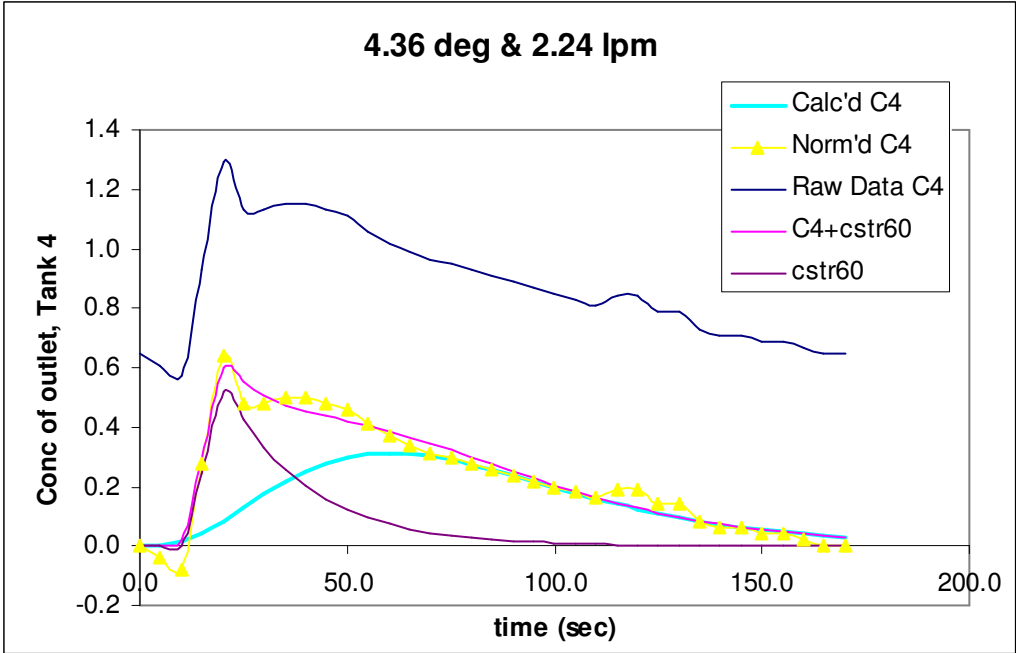


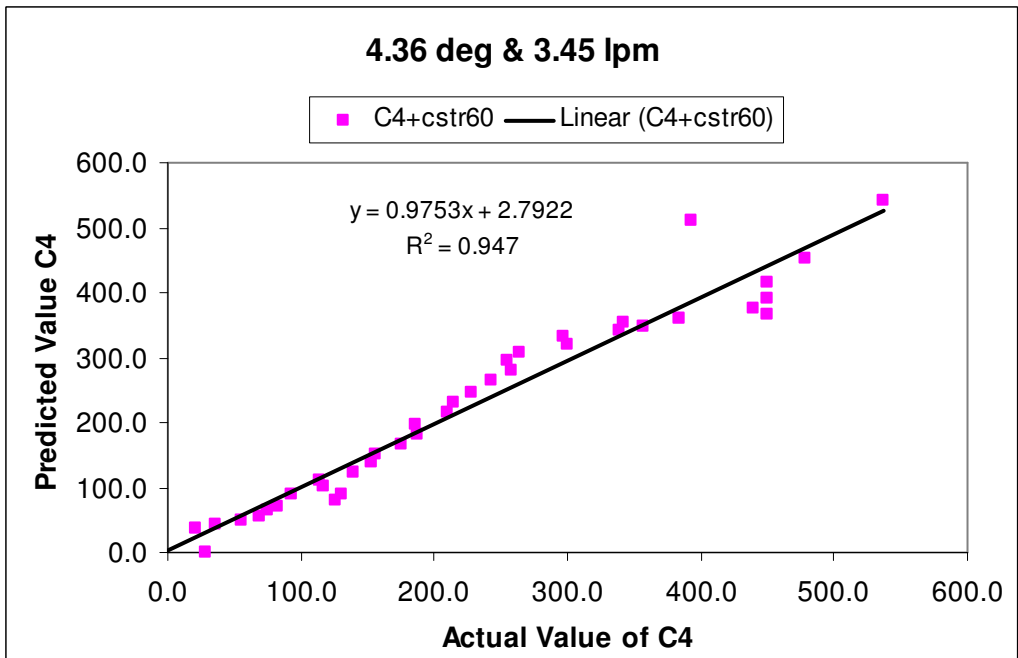
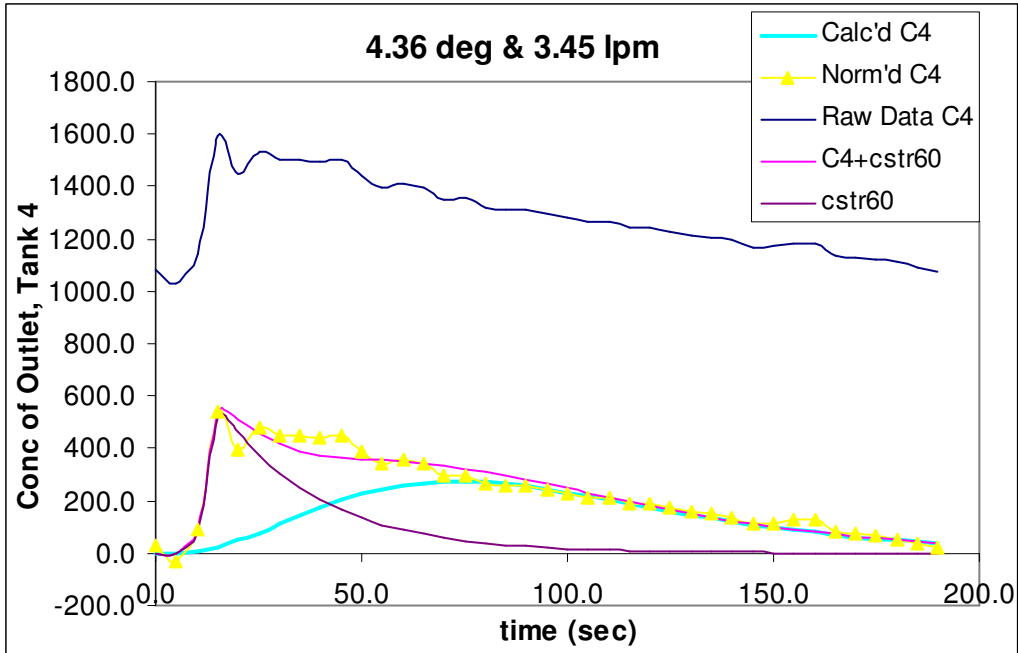
Volume as a Function of the Angle of Inclination

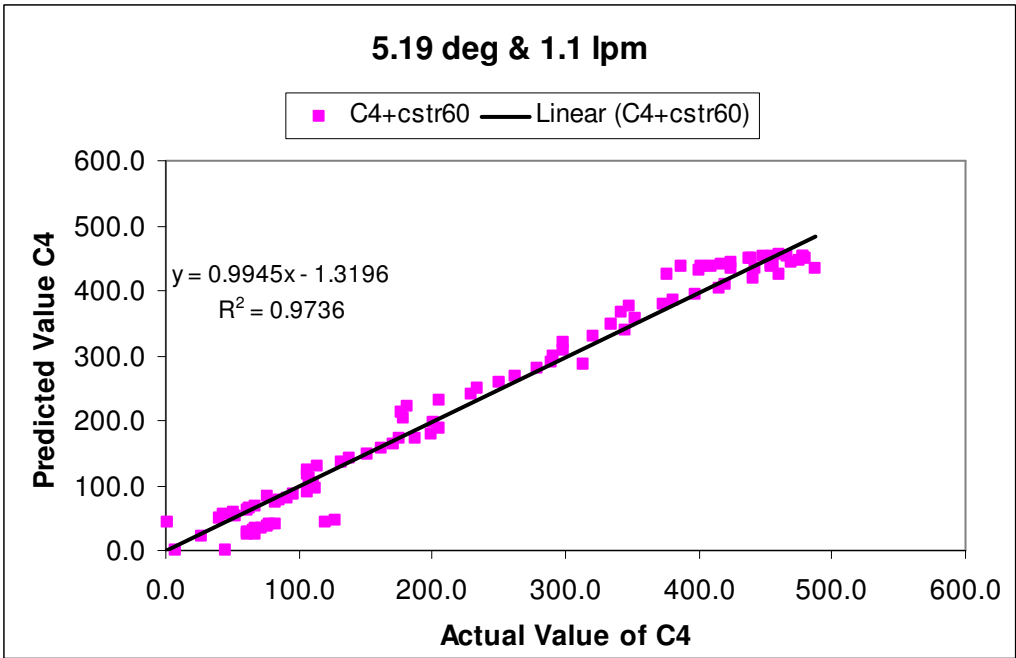
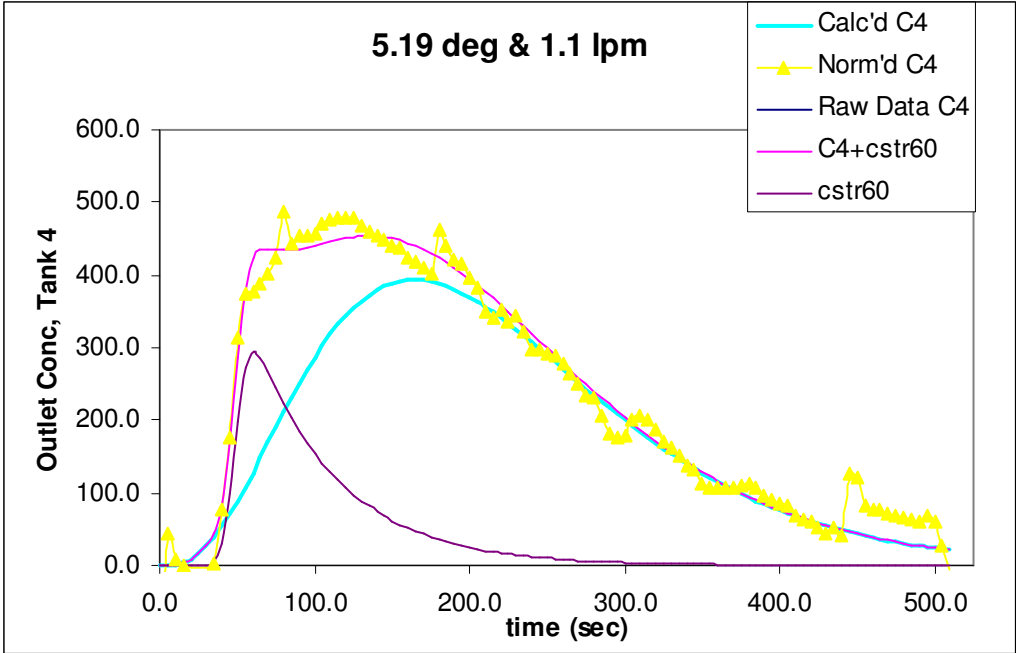


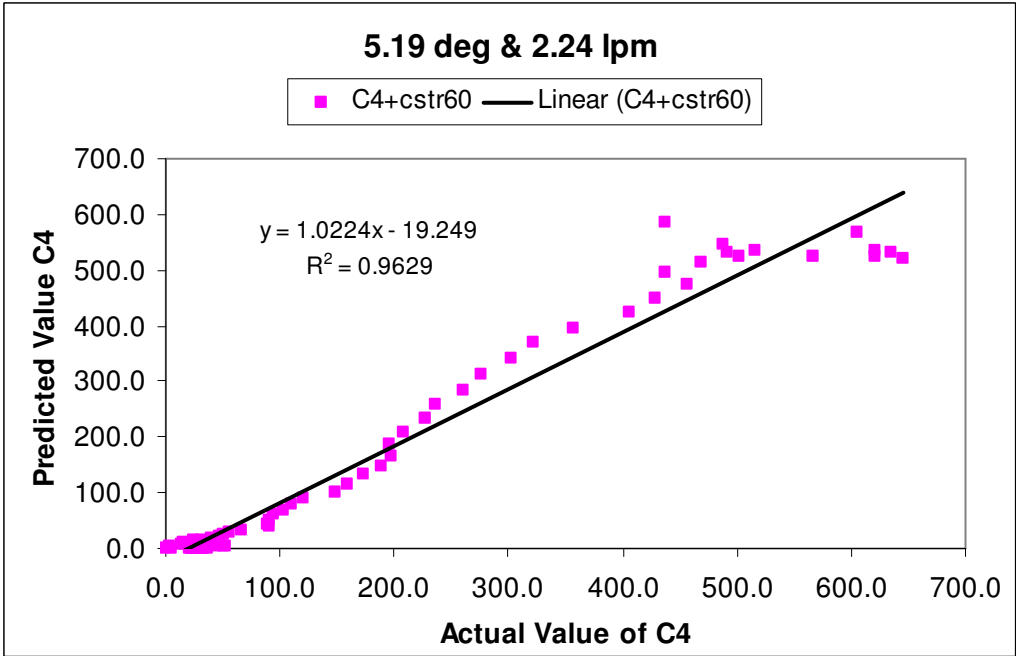
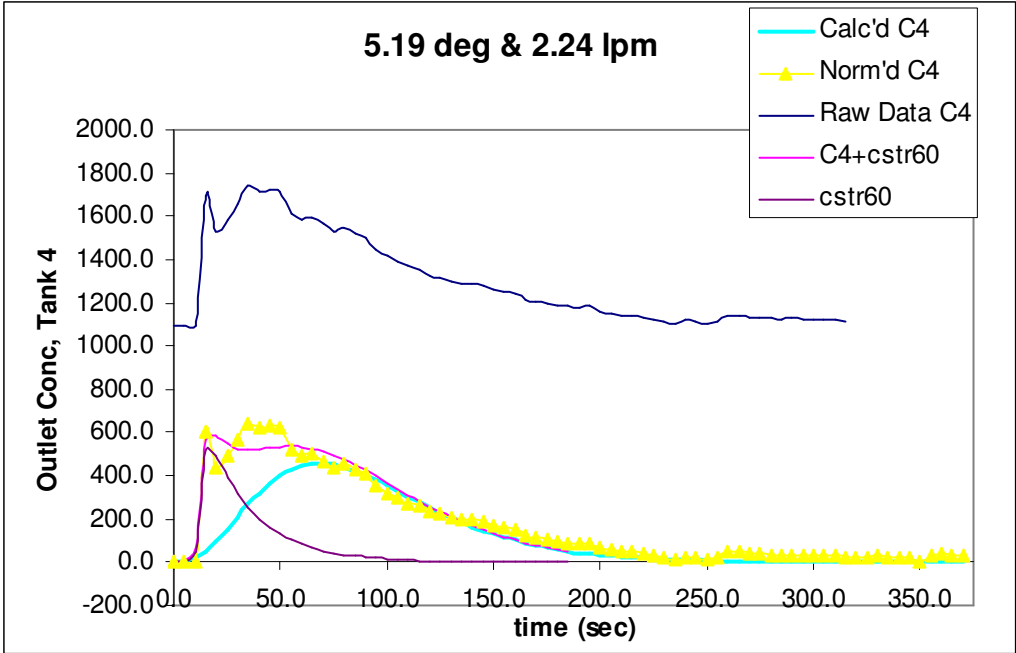
Conductivity Data for Given Flow Conditions

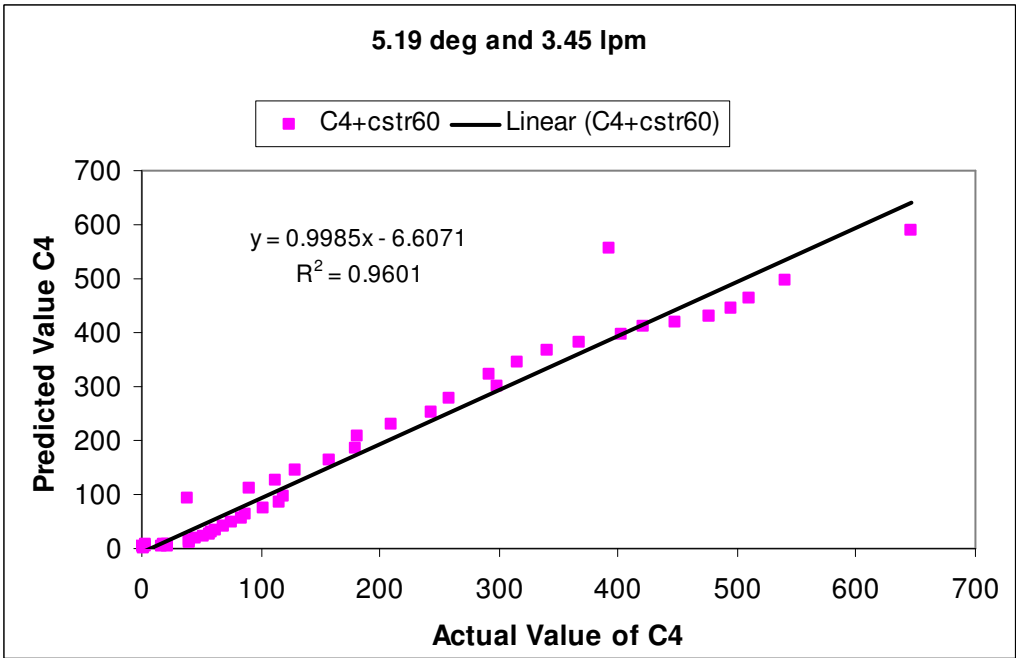
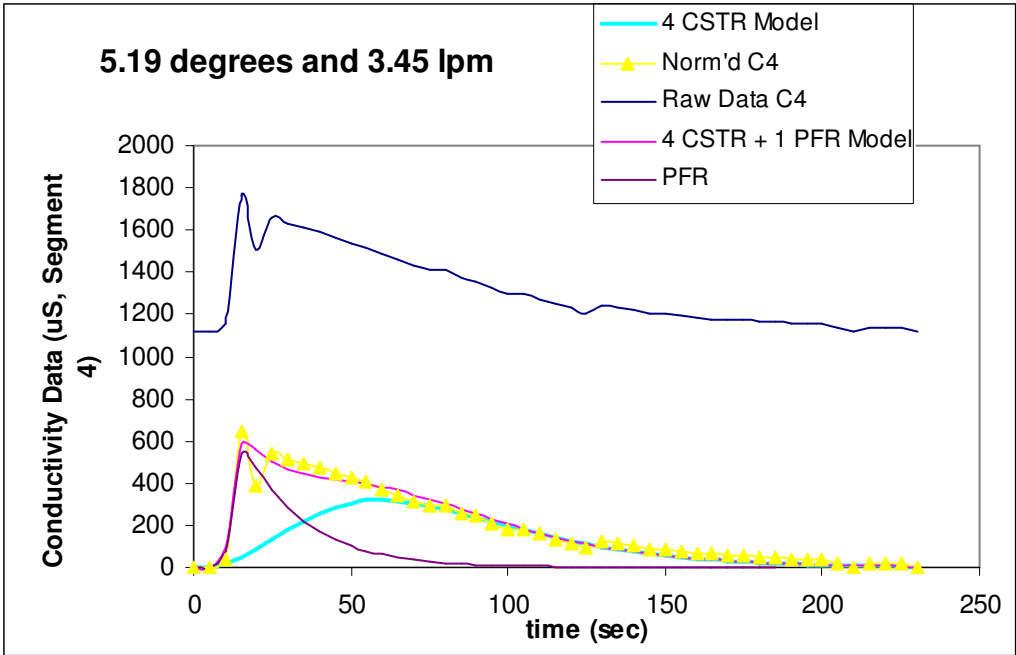


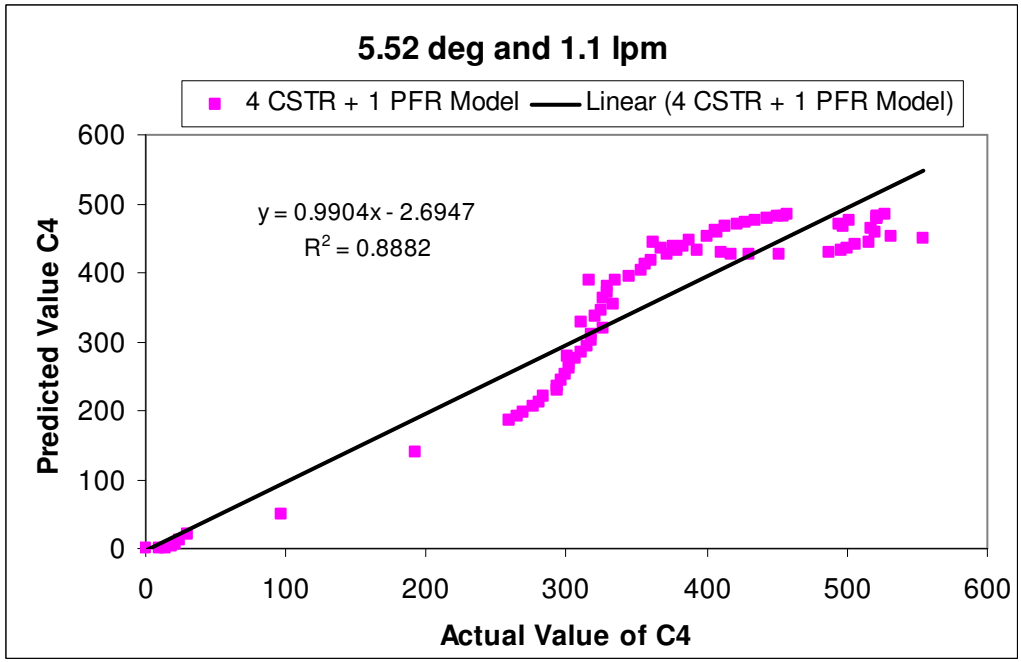
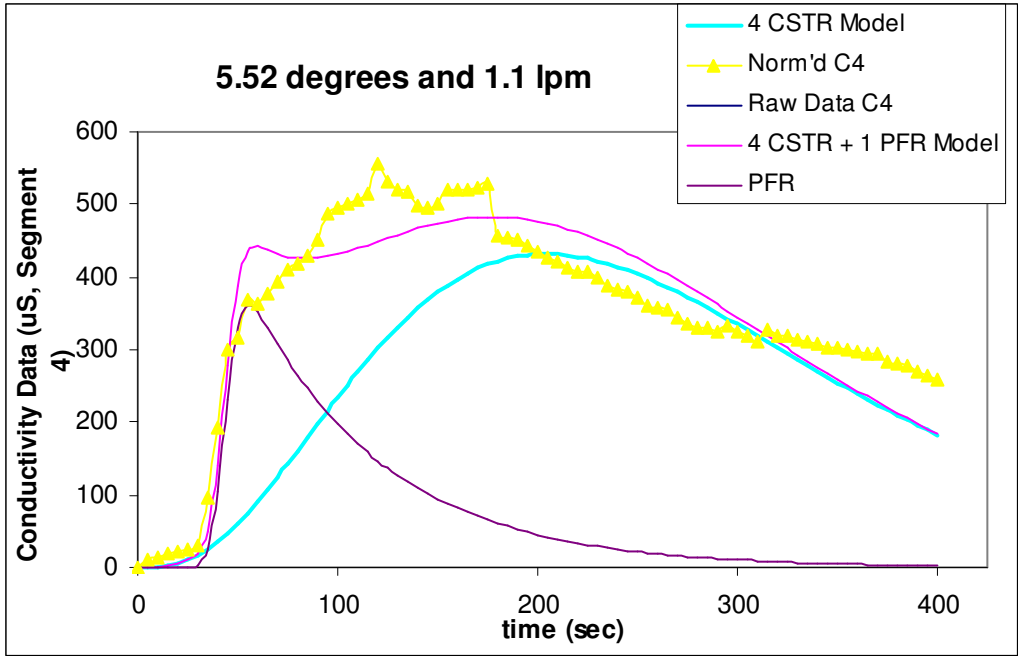


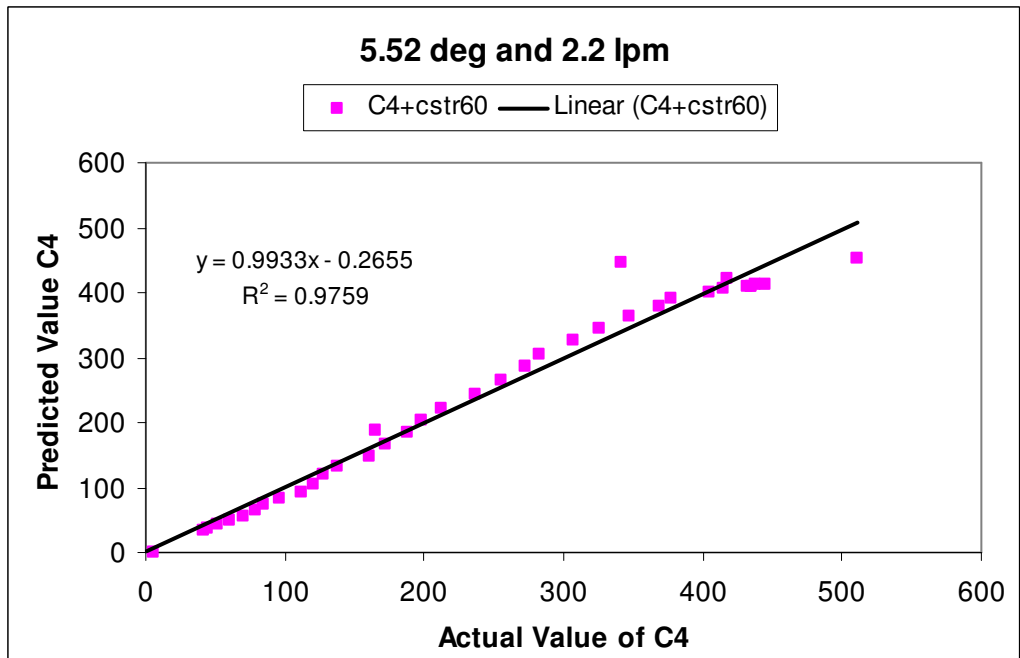
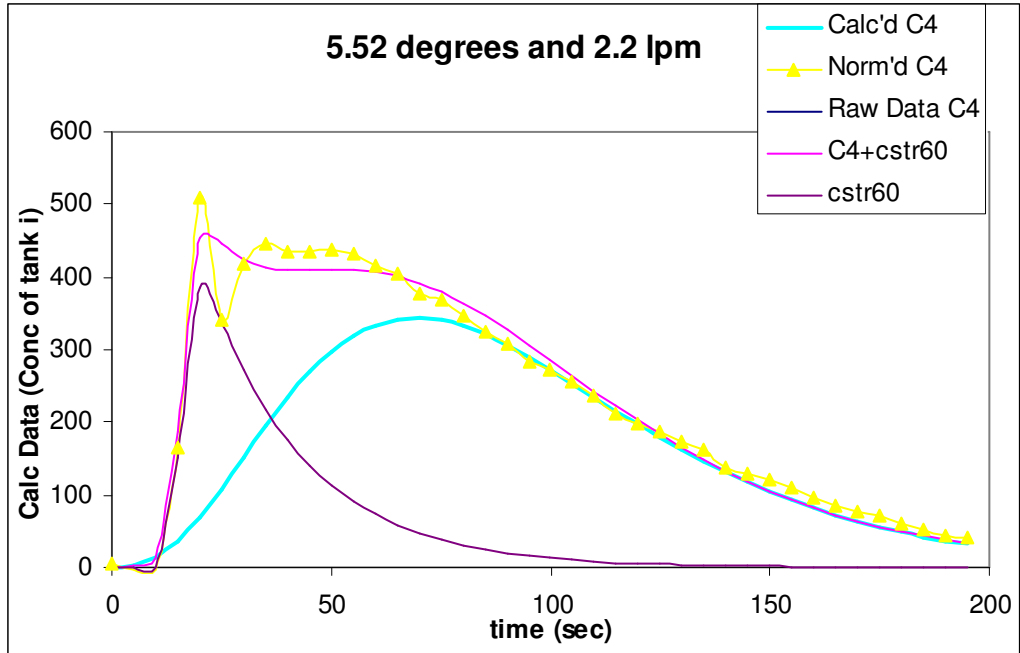


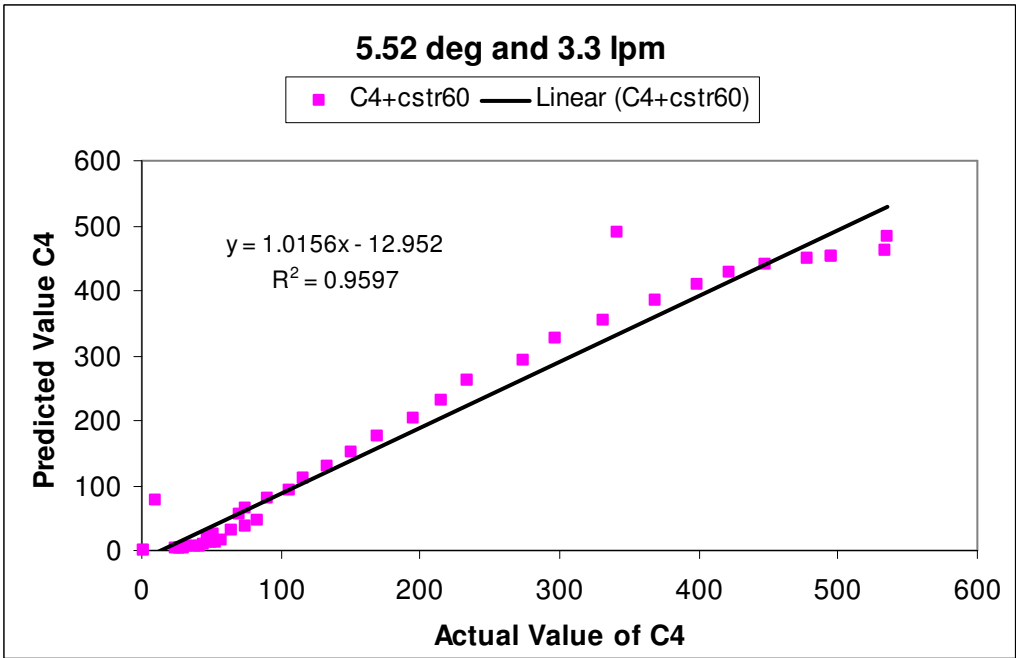
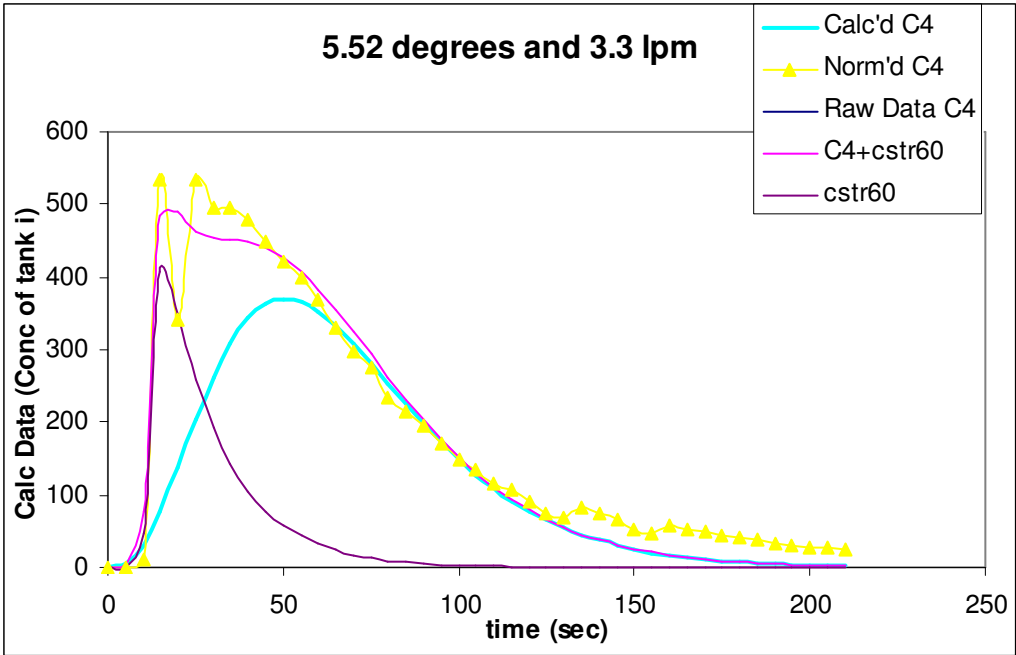


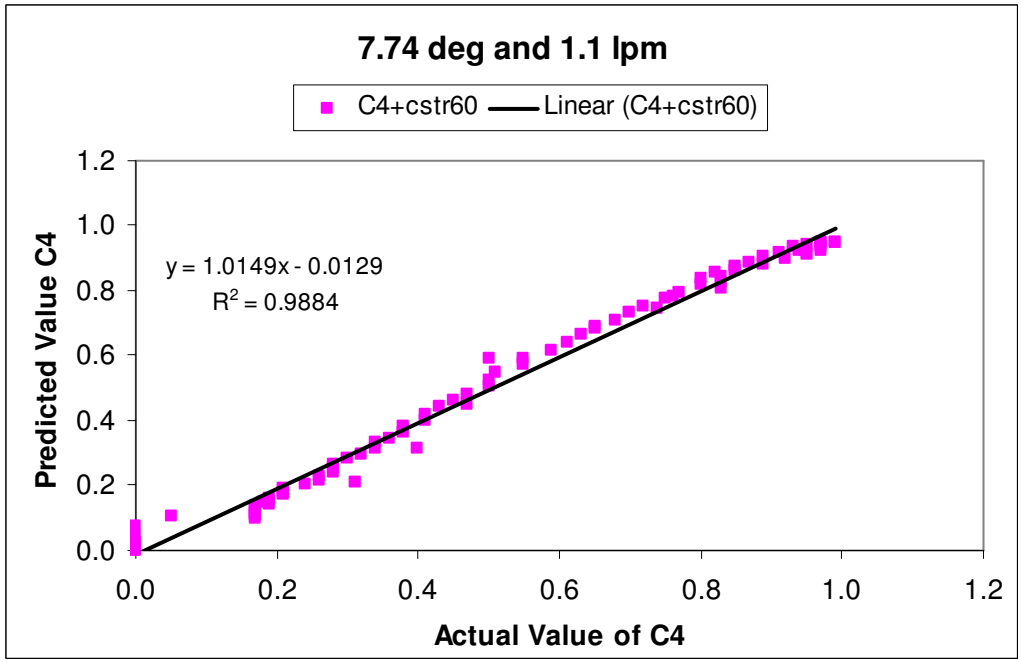
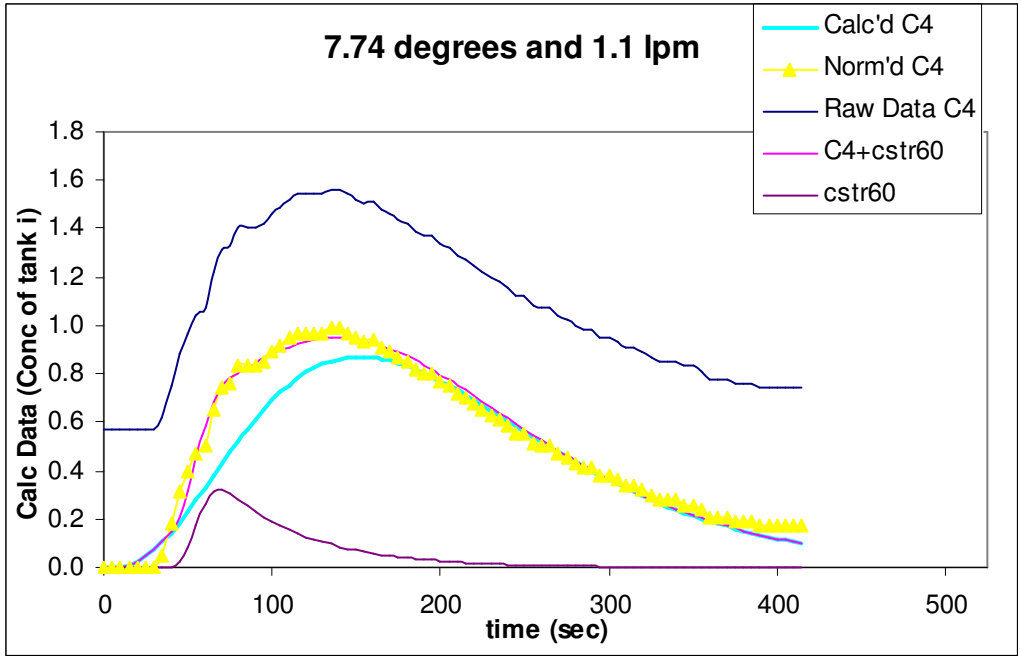


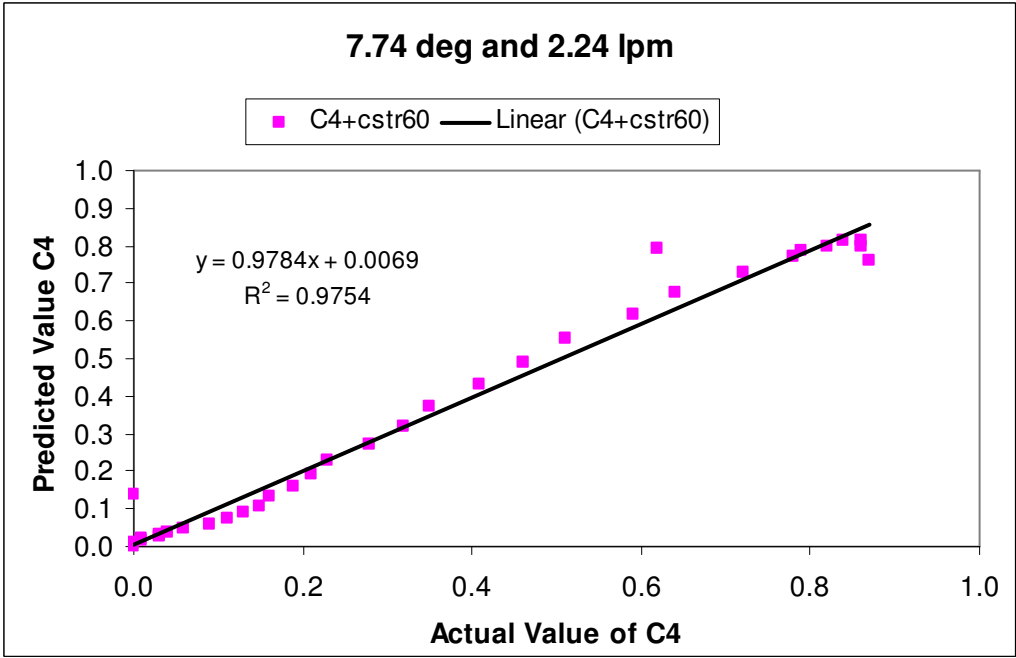
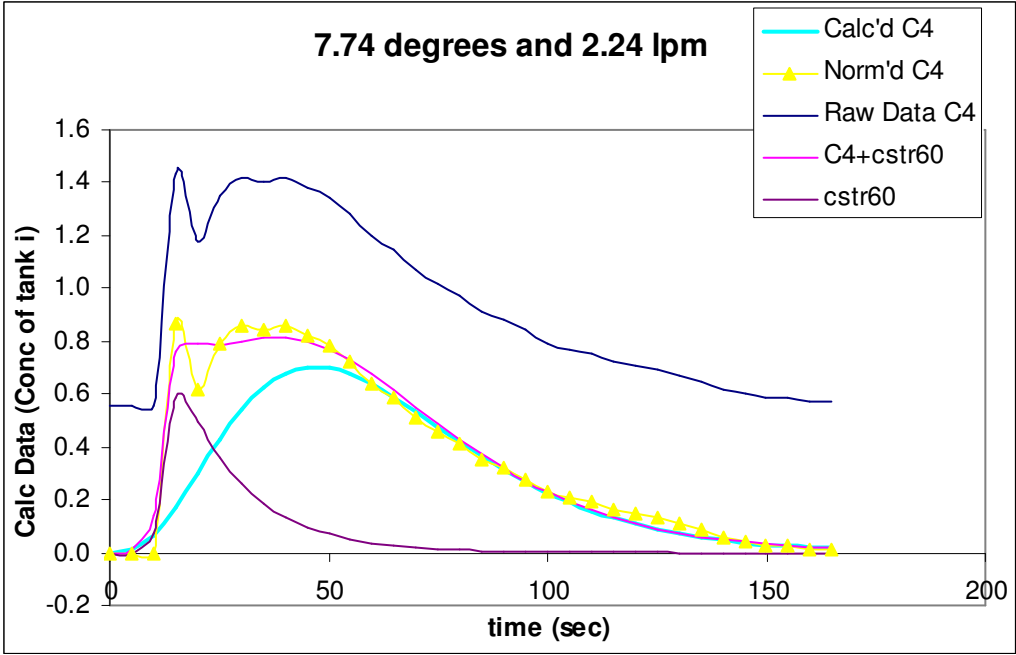


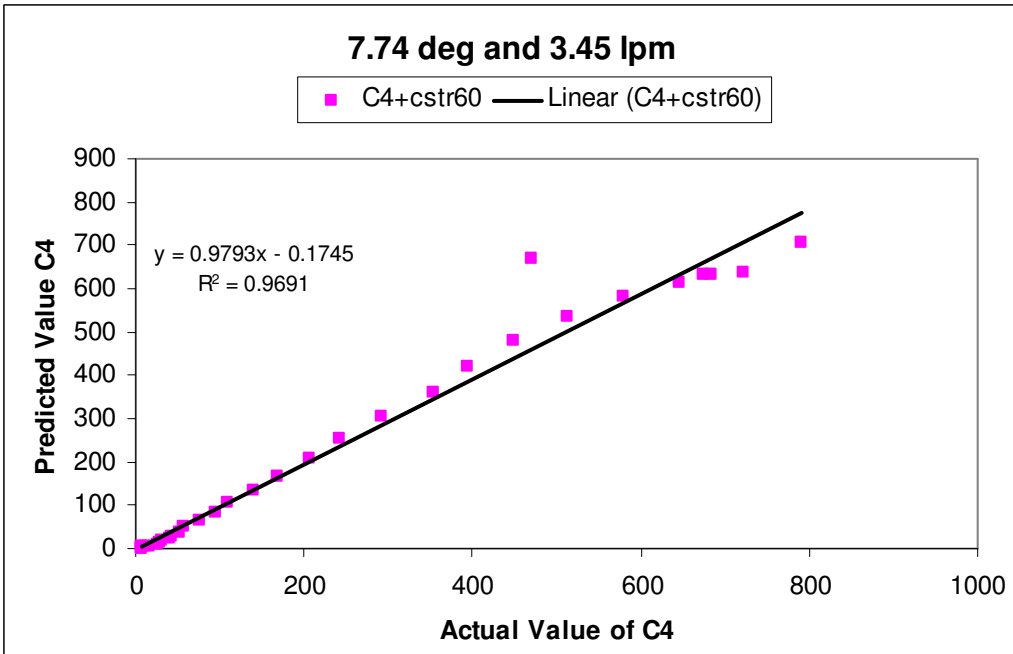
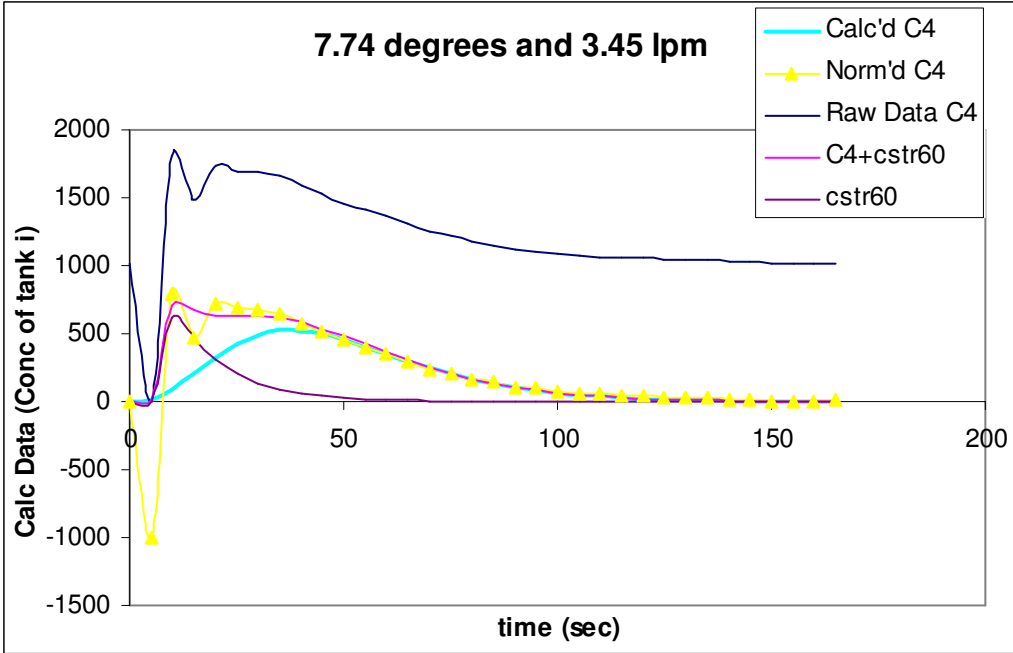


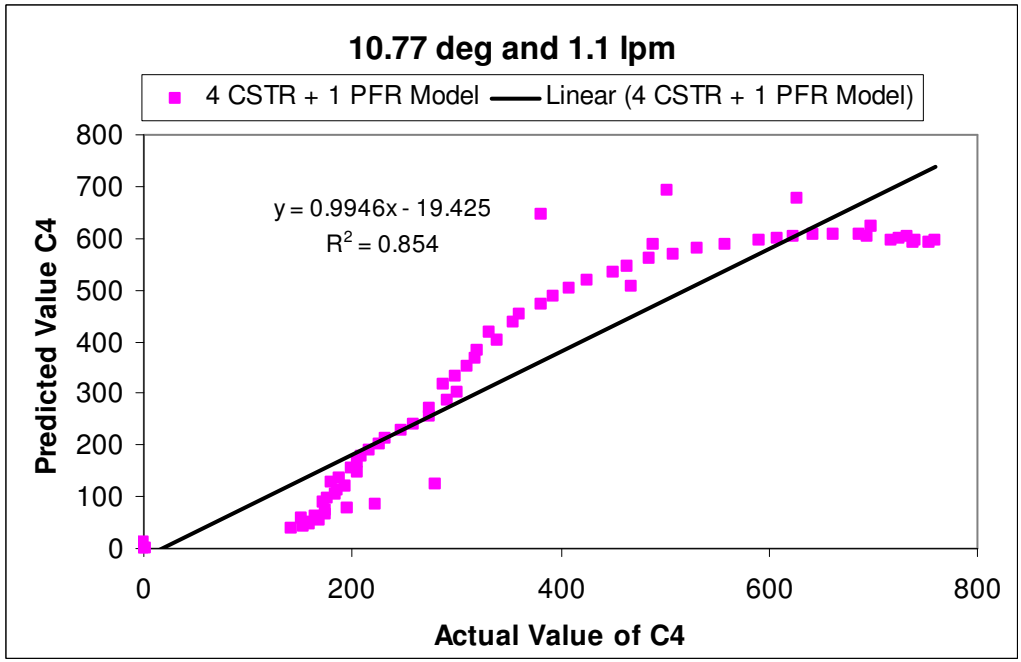
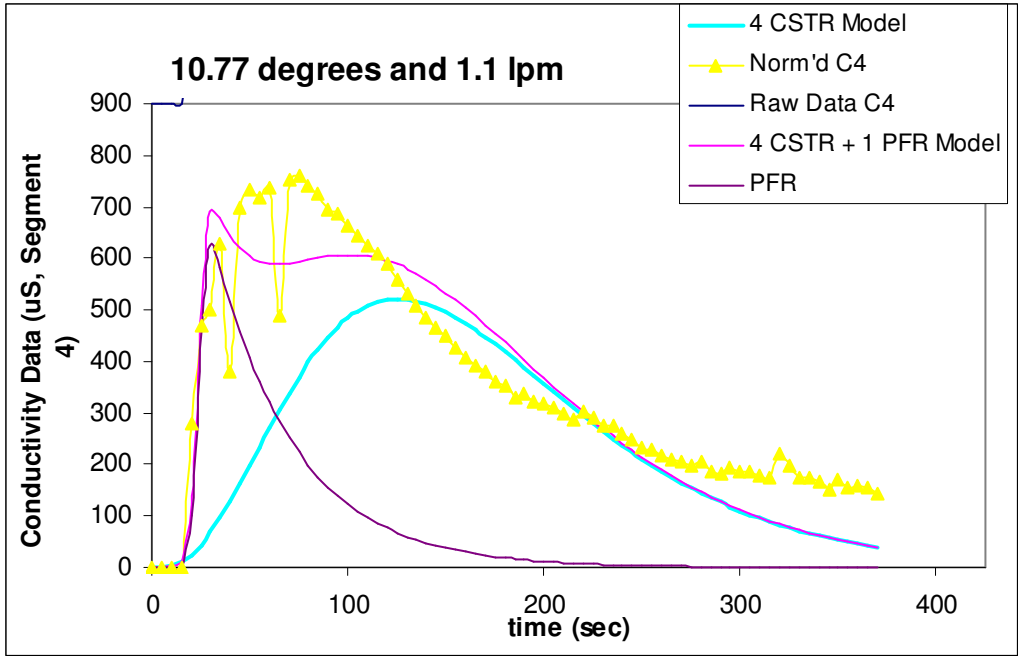


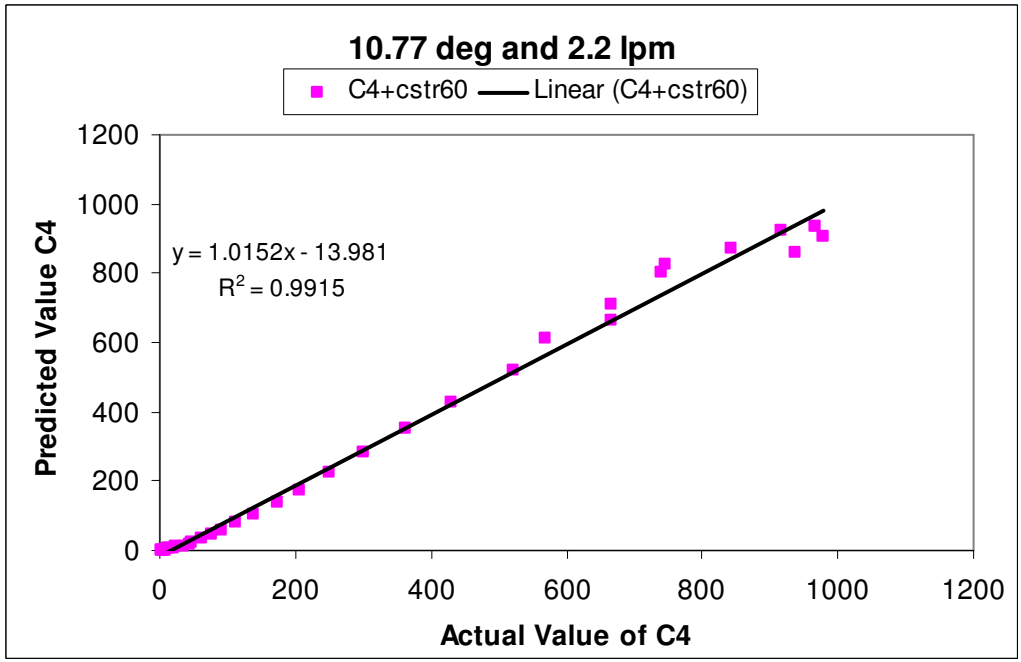
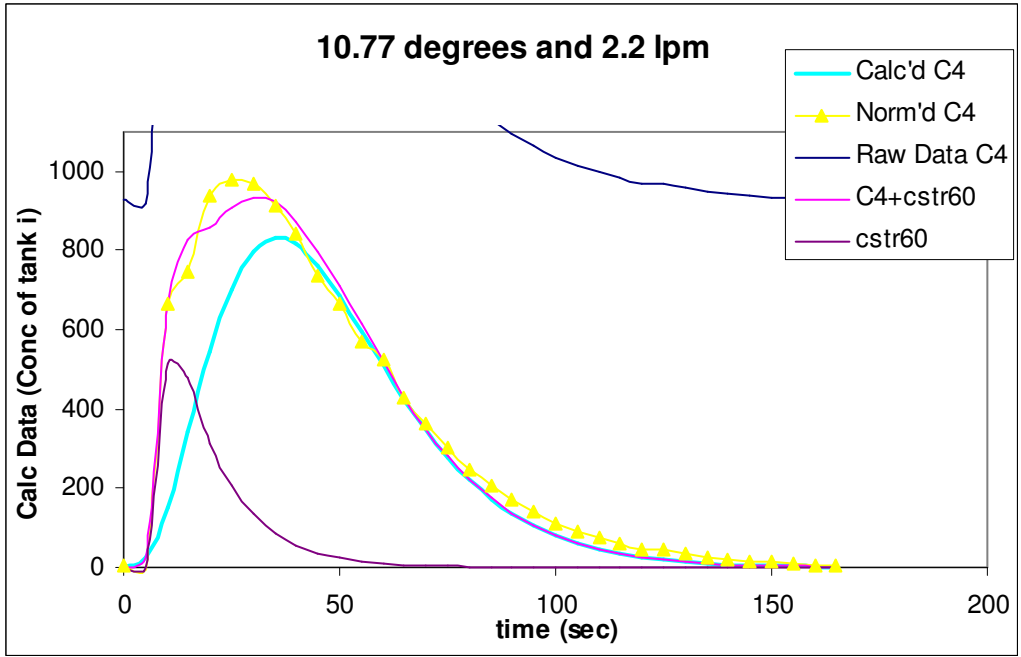


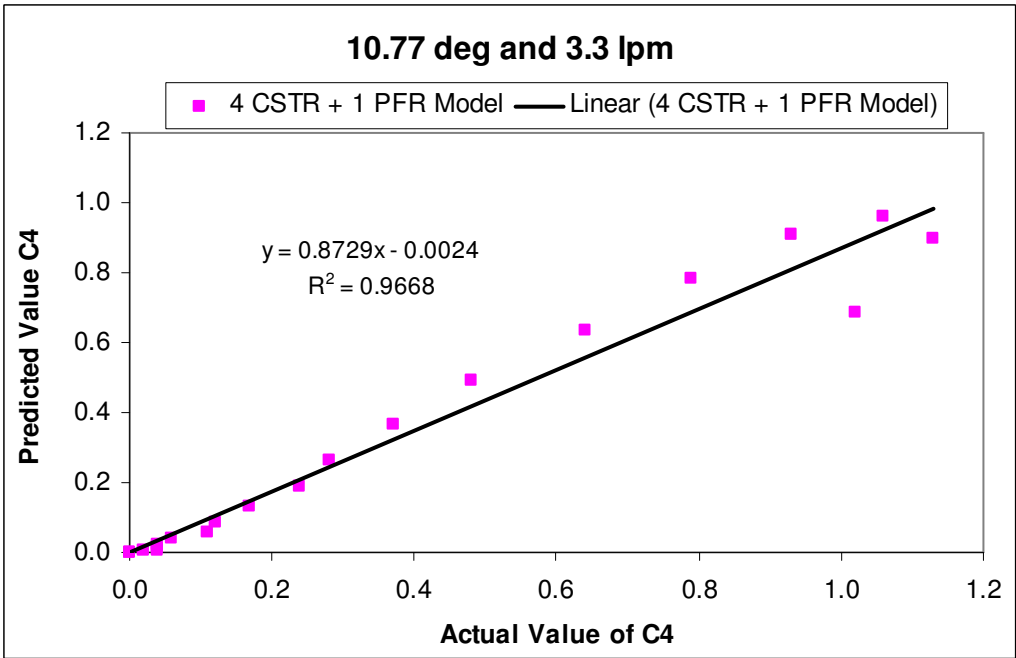
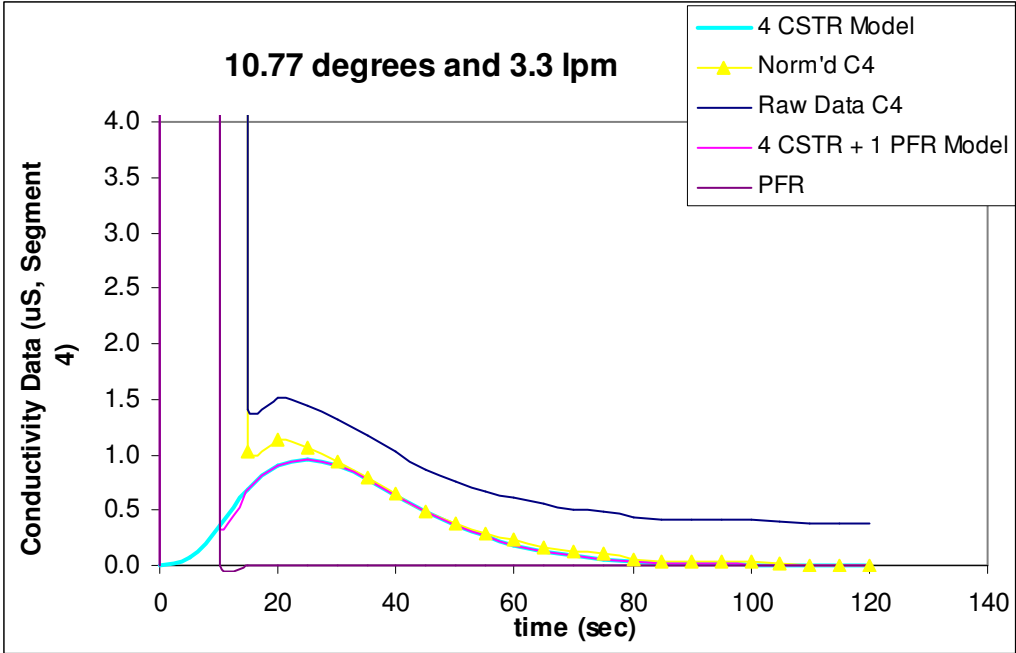












R² and R²-Adjusted Calculations

- R²:

$$R^2 = 1 - \frac{SSE}{SST}$$

$$SSE = \sum_i (y_i - \hat{y}_i)^2$$

$$SST = \sum_i (y_i - \bar{y})^2$$

- R²-Adj (adjusts for inflation of R² due to number of parameters in a model):

$$R^2 Adj = 1 - (1 - R^2) * \frac{(n - 1)}{(n - p - 1)}$$

Where n is the number of data points and p is the number of parameters in the model